6

Potential Climate Change from Aviation

MICHAEL PRATHER AND ROBERT SAUSEN

Lead Authors:
A.S. Grossman, J.M. Haywood, D. Rind, B.H. Subbaraya

Contributors:
P. Forster, A. Jain, M. Ponater, U. Schumann, W.-C. Wang, T.M.L. Wigley, D.J. Wuebbles

Review Editor:
D. Yihui

CONTENTS

EXECUTIVE SUMMARY

- Aircraft emissions in conjunction with other anthropogenic sources are expected to modify atmospheric composition (gases and aerosols), hence radiative forcing and climate. Atmospheric changes from aircraft result from three types of processes: direct emission of radiatively active substances (e.g., CO_2 or water vapor); emission of chemical species that produce or destroy radiatively active substances (e.g., NO_x, which modifies O_3 concentration); and emission of substances that trigger the generation of aerosol particles or lead to changes in natural clouds (e.g., contrails).

- Radiative forcing (RF) is the metric used here (and in IPCC) to compare climate perturbations among different aviation scenarios and with total anthropogenic climate change. RF is the global, annual mean radiative imbalance to the Earth's climate system caused by human activities. It predicts changes to the global mean surface temperature: Positive RF leads to global warming. Yet climate does not change uniformly; some regions warm or cool more than others; and mean temperature does not describe vital aspects of climate change such as droughts and severe storms. Aviation's impacts via O_3 and contrails occur predominantly in northern mid-latitudes and the upper troposphere, leading potentially to climate change of a different nature than that from CO_2. Nevertheless, we follow the scientific basis for RF from IPCC's Second Assessment Report and take summed RF as a first-order measure of global mean climate change.

- For the 1992 aviation scenario (NASA-1992*), radiative forcing of climate change from aircraft emissions (gases and aerosols) is estimated to be +0.05 W m^{-2}, which is about 3.5% of total anthropogenic radiative forcing as measured against the pre-industrial atmosphere of +1.4 W m^{-2} for combined greenhouse gases and aerosols (and +2.7 W m^{-2} for greenhouse gases alone). The components of aircraft-induced radiative forcing are as follows: CO_2, +0.018 W m^{-2}; NO_x, +0.023 W m^{-2} (via ozone changes) and -0.014 W m^{-2} (via methane changes); contrails, +0.02 W m^{-2}; stratospheric H_2O, +0.002 W m^{-2}; sulfate aerosol (direct effect), -0.003 W m^{-2}; and black carbon aerosol (soot), +0.003 W m^{-2}. Changes in "natural" cirrus clouds caused by aircraft may result in negligible or potentially large radiative forcing; an estimate could fall between 0 and 0.04 W m^{-2}. Uncertainty estimates, typically a factor of 2 or 3, have been made for individual components and are intended to represent consistent confidence intervals that the radiative forcing value is likely (2/3 of the time) to fall within the range shown. The uncertainty estimate for the total radiative forcing (without additional cirrus clouds) is calculated as the square root of the sums of the squares of the upper and lower ranges of the individual components.

- Projection of subsonic fleet growth to 2015 (NASA-2015* scenario) results in a best estimate for total aircraft-induced radiative forcing of +0.11 W m^{-2} in 2015—about 5% of IS92a projected radiative forcing from all anthropogenic emissions that year.

- Various options for the future development of subsonic air traffic under the International Civil Aviation Organization (ICAO)-developed Forecasting and Economic Subgroup (FESG, or F-type) scenarios for aviation in the year 2050 assume an increase in fuel use by 2050 relative to 1992 by a factor of 1.7 to 4.8. These options result in a range for aircraft-induced total radiative forcing (without additional cirrus clouds) from +0.13 to +0.28 W m^{-2} in 2050, or 3–7% of IS92a total anthropogenic radiative forcing for that year. However, the upper and lower bounds represent aircraft scenarios that diverge significantly from economic growth assumed for IS92a. Alternative Environmental Defense Fund (EDF, or E-type) scenarios considered here adopt growth in 2050 fuel use by factors of 7 to more than 10 and result in a range of total radiative forcing (without additional cirrus clouds) from +0.4 to +0.6 W m^{-2}.

- For the year 2050, a scenario that matches IS92a economic growth (scenario Fa1) gives total radiative forcing of +0.19 W m^{-2}. Individual contributions to aircraft-induced radiative forcing are as follows: CO_2, +0.074 W m^{-2}; NO_x, +0.060 W m^{-2} (via ozone changes) and -0.045 W m^{-2} (via methane changes); contrails, +0.10 W m^{-2}; stratospheric H_2O, +0.004 W m^{-2}; sulfate aerosols (direct effect), -0.009 W m^{-2}; and black carbon aerosols (soot), +0.009 W m^{-2}. The contrail estimate includes an increase in fuel consumption, higher overall efficiency of propulsion (i.e., cooler exhaust), and shifting of routes. An estimate for the radiative forcing from additional cirrus could fall between 0 and 0.16 W m^{-2}.

- As one option for future aviation, we consider the addition of a fleet of high-speed civil transport (HSCT, supersonic) aircraft replacing part of the subsonic air traffic under scenario Fa1. In this example, HSCT aircraft are assumed to begin operation in the year 2015, to grow linearly to a maximum of 1,000 aircraft by the year 2040, and to use new technologies to maintain very low emissions of 5 g NO_2 per kg fuel. By the year 2050, this combined fleet

(scenario Fa1H) would add 0.08 W m^{-2} on top of the 0.19 W m^{-2} radiative forcing from scenario F1a. This additional radiative forcing combines direct HSCT effects with the reduction in equivalent subsonic air traffic: +0.006 Wm^{-2} from additional CO_2, +0.10 W m^{-2} from increased stratospheric H_2O, -0.012 W m^{-2} from ozone and methane changes resulting from NO_x emissions, and -0.011 W m^{-2} from reduced contrails. In total, the best value for HSCT RF is about 5 times larger than that of displaced subsonic aircraft, although the recognized uncertainty includes a factor as small as zero. The RFs from changes in stratospheric H_2O and O_3 are difficult to simulate in models and remain highly uncertain.

- Although the task of detecting climate change from all human activities is already difficult, detecting the aircraft-specific contribution to global climate change is not possible now and presents a serious challenge for the next century. Aircraft radiative forcing, like forcing from other individual sectors, is a small fraction of the whole anthropogenic climate forcing: about 4% today and by the year 2050 reaching 3–7% for F-type scenarios and 10–15% for E-type scenarios.

- The Radiative Forcing Index (RFI)—the ratio of total radiative forcing to that from CO_2 emissions alone—is a measure of the importance of aircraft-induced climate change other than that from the release of fossil carbon alone. In 1992, the RFI for aircraft is 2.7; it evolves to 2.6 in 2050 for the Fa1 scenario. This index ranges from 2.2 to 3.4 for the year 2050 for various E- and F-type scenarios for subsonic aviation and technical options considered here. The RFI increases from 2.6 to 3.4 with the addition of HSCTs (scenario Fa1H), primarily as a result of the effects of stratospheric water vapor. Thus, aircraft-induced climate change with RFI > 1 points to the need for a more thorough climate assessment for this sector. By comparison, in the IS92a scenario the RFI for all human activities is about 1, although for greenhouse gases alone it is about 1.5, and it is even higher for sectors emitting CH_4 and N_2O without significant fossil fuel use.

- From 1990 to 2050, the global mean surface temperature is expected to increase by 0.9 K following scenario IS92a for all human activity (assuming a climate sensitivity of +2.5 K for doubling of CO_2). Aircraft emissions from subsonic fleet scenario Fa1 are estimated to be responsible for about 0.05 K of this temperature rise.

- At present, the largest aircraft forcings of climate are through CO_2, NO_x, and contrail formation. These components have similar magnitude for subsonic aircraft; for an HSCT fleet, H_2O perturbations in the lower stratosphere, which are the most uncertain, are the most important. The largest areas of scientific uncertainty in predicting aircraft-induced climate effects lie with persistent contrails, with tropospheric ozone increases and consequent changes in methane, with potential particle impacts on “natural” clouds, and with water vapor and ozone perturbations in the lower stratosphere (especially for supersonic transport).

- The advantages of low-NO_x engines (scenario Fa2) are calculated to be modest in terms of total radiative forcing by the year 2050. The climatic impact of technology options, which in these scenarios are phased in linearly between 2015 and 2050, would not be fully felt until after 2050. Although lower NO_x emissions ameliorate the aviation-induced build-up of tropospheric O_3 and its radiative forcing as expected, they also reduce the opposite-sign radiative forcing associated with lowered global CH_4 abundance. The prospect of large canceling RFs, each with large uncertainties, greatly increases the probability of a large residual. Furthermore, RF is a measure only of *global* mean warming. Aircraft O_3 and CH_4 changes have largely different latitudinal contributions to RF; although they partly cancel on average, they may induce *regional* climate change.

6.1. How Do Aircraft Cause Climate Change?

Aircraft perturb the atmosphere by changing background levels of trace gases and particles and by forming condensation trails (contrails). Aircraft emissions include greenhouse gases such as CO_2 and H_2O that trap terrestrial radiation and chemically active gases that alter natural greenhouse gases, such as O_3 and CH_4. Particles may directly interact with the Earth's radiation balance or influence the formation and radiative properties of clouds. Figure 6-1 portrays a causal chain whereby the direct emissions of aircraft accumulate in the atmosphere, change the chemistry and the microphysics, and alter radiatively active substances in the atmosphere, which change radiative forcing and hence the climate.

Chapters 2 and 3 link the direct emissions of aircraft today to changes in radiatively active substances, and Chapter 4 projects these atmospheric changes into the future for a range of aviation scenarios. This chapter presents calculations of radiative forcing from aircraft-related atmospheric changes and discusses implications concerning the role of aircraft in a changing climate. This section begins with the concept of "dangerous climate change," as defined within the mandate of the United Nations Framework Convention on Climate Change (FCCC), then presents the IS92 scenarios for future climate change associated with the Second Assessment Report (IPCC, 1996). Section 6.1 also summarizes aviation's potential role in climate change and its proportion of fossil fuel use. Section 6.2 discusses the concepts of radiative forcing (RF) and global warming potential (GWP). Section 6.3 provides calculations of radiative forcing from aircraft perturbation of greenhouse gases, and Section 6.4 presents calculations of RF from aircraft perturbations of aerosols and contrails. Section 6.5 examines how radiative forcing can be used as a predictor of climate change and presents some case studies of climate change patterns that might be induced by aviation. Finally, Section 6.6 presents the summed radiative forcing, and associated climate change, for a range of projected scenarios and technological options in future aviation.

6.1.1. Anthropogenic Climate Change, Variability, and Detection

What is climate change? The common definition of climate refers to the average of weather, yet the definition of the climate system must reach out to the broader geophysical system that interacts with the atmosphere and our weather. The concept of climate change has acquired a number of different meanings in the scientific literature and in the media. Often, "climate change" denotes variations resulting from human interference, and "climate variability" refers to natural variations. Sometimes "climate change" designates variations longer than a certain period. Finally, "climate change" is often taken to mean climate fluctuations of a global nature, including effects from human activities such as the enhanced greenhouse effect and from natural causes such as volcanic aerosols.

For the purposes of the UNFCCC (and this report), the definition of climate change is: "A change of climate which is attributed directly or indirectly to human activity that alters the composition of the global atmosphere and which is in addition to natural climate variability observed over comparable time periods." This alteration of the global atmosphere includes changes in land use as well as anthropogenic emissions of greenhouse

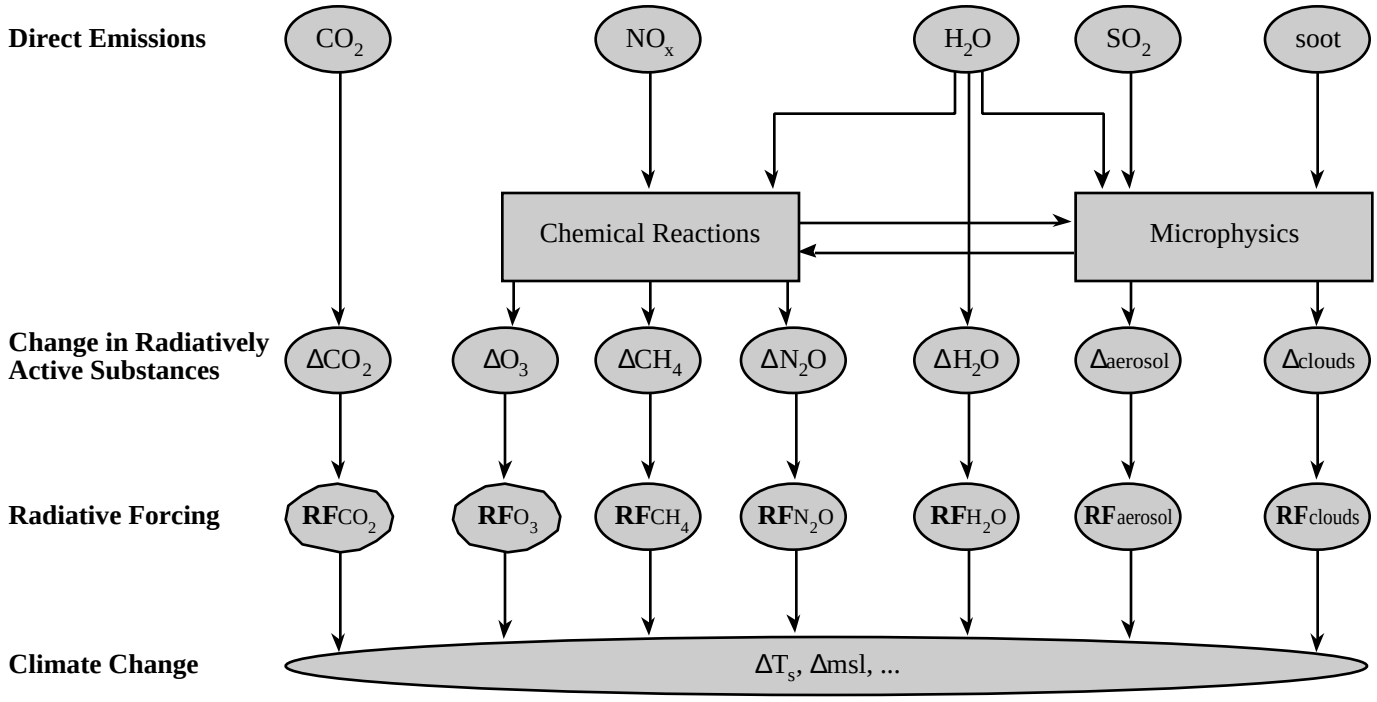

Figure 6-1: Schematic of possible mechanisms whereby aircraft emissions impact climate. Climate impact is represented by changes in global mean surface temperature (ΔT_s) and global mean sea level rise (Δmsl).

gases and particles. This FCCC definition thus introduces the concept of the difference between the effect of human activities (climate change) and climatic effects that would occur without such human interference (climate variability).

What drives changes in climate? The Earth absorbs radiation from the sun, mainly at the surface. This energy is then redistributed by atmospheric and oceanic circulations and radiated to space at longer ("terrestrial" or "infrared") wavelengths. On average, for the Earth as a whole, incoming solar energy is balanced by outgoing terrestrial radiation. Any factor that alters radiation received from the sun or lost to space or the redistribution of energy within the atmosphere and between atmosphere, land, and ocean can affect climate. A change in radiative energy available to the global Earth/atmosphere system is termed here, as in previous IPCC reports, radiative forcing (see Section 6.2 for more details). Radiative forcing (RF) is the global, annual average of radiative imbalance (W m^{-2}) in net heating of the Earth's lower atmosphere as a result of human activities since the beginning of the industrial era almost 2 centuries ago.

Increases in the concentrations of greenhouse gases reduce the efficiency with which the surface of the Earth radiates heat to space: More outgoing terrestrial radiation from the surface is absorbed by the atmosphere and is emitted at higher altitudes and colder temperatures. This process results in positive radiative forcing, which tends to warm the lower atmosphere and the surface. This radiative forcing is the enhanced greenhouse effect—an enhancement of an effect that has operated in the Earth's atmosphere for billions of years as a result of naturally occurring greenhouse gases (i.e., water vapor, carbon dioxide, ozone, methane, and nitrous oxide). The amount of warming depends on the size of the increase in concentration of each greenhouse gas, the radiative properties of the gases involved, their geographical and vertical distribution, and the concentrations of other greenhouse gases already present in the atmosphere.

Anthropogenic aerosols (small particles and droplets) in the troposphere—derived mainly from the emission of sulfur dioxide from fossil fuel burning but also from biomass burning and aircraft—can absorb and reflect solar radiation. In addition, changes in aerosol concentrations may alter cloud amount and cloud reflectivity through their effect on cloud microphysical properties. Often, tropospheric aerosols tend to produce negative radiative forcing and thus to cool climate. They have a much shorter lifetime (days to weeks) than most greenhouse gases (which have lifetimes of decades to centuries), so their concentrations respond much more quickly to changes in emissions.

Other natural changes, such as major volcanic eruptions that produce extensive stratospheric aerosols or variations in the sun's energy output, also drive climate variation by altering the radiative balance of the planet. On time scales of tens of thousands of years, slow variations in the Earth's orbit, which are well understood, have led to changes in the seasonal and latitudinal distribution of solar radiation; these changes have played an important part in controlling variations of climate in the distant past, such as glacial cycles.

Any changes in the radiative balance of the Earth, including those resulting from an increase in greenhouse gases or aerosols, will tend to alter atmospheric and oceanic temperatures and associated circulation and weather patterns. These effects will be accompanied by changes in the hydrological cycle (for example, altered cloud distributions or changes in rainfall and evaporation regimes). Any human-induced changes in climate will also alter climatic variability that otherwise would have occurred. Such variability contains a wide range of space and time scales. Climate variations can also occur in the absence of a change in external forcing, as a result of complex interactions between components of the climate system such as the atmosphere and ocean. The El Niño-Southern Oscillation (ENSO) phenomenon is a prominent example of such natural "internal" variability.

In the observationally based record of global mean surface temperatures shown by the black line on Figure 6-2, both interannual variability and a positive trend are apparent. Year-to-year variations can be interpreted as resulting from internal variability; and the trend, as caused by external forcing mechanisms. For comparison, the yellow line on Figure 6-2 shows a control run from a coupled ocean-atmosphere general circulation model in which concentrations of greenhouse gases and aerosols are held fixed: This indicates that observed natural variability in global mean surface temperatures may be adequately simulated. The red and the blue lines in Figure 6-2 show the surface temperature simulated by two different general circulation models driven by increased greenhouse gas and sulfate aerosol concentrations. Both of the models simulate interannual variability and trends in surface temperature, but differences in model sensitivities (see Section 6.2) lead to differing temperature trends. Figure 6-2 also shows that estimates of the global mean temperature trend resulting from increased greenhouse gas concentrations alone (green line) leads to a larger temperature change than observed.

It is difficult to ascribe climate change to human activities and even harder to identify a particular change with a specific activity. The point at which change is detected in a climate variable is the point at which the observed global mean trend (signal) unambiguously rises above background natural climate variability (noise). Good observational records of climate and sufficiently accurate, reliable models are needed. To simulate climate change, the models require complete representation of all anthropogenic forcing mechanisms (i.e., changes in atmospheric composition). In practice, current climate change is just comparable to natural variability. Therefore, more sophisticated tools have been developed that use the spatial structure of specific climate variables expected to change, which is known as the "fingerprint" method of detection (e.g., Hasselmann, 1993; Santer *et al*., 1996).

6.1.2. Aircraft-Induced Climate Change

Aircraft emissions are expected to modify the Earth's radiative budget and climate as a result of several processes (see also

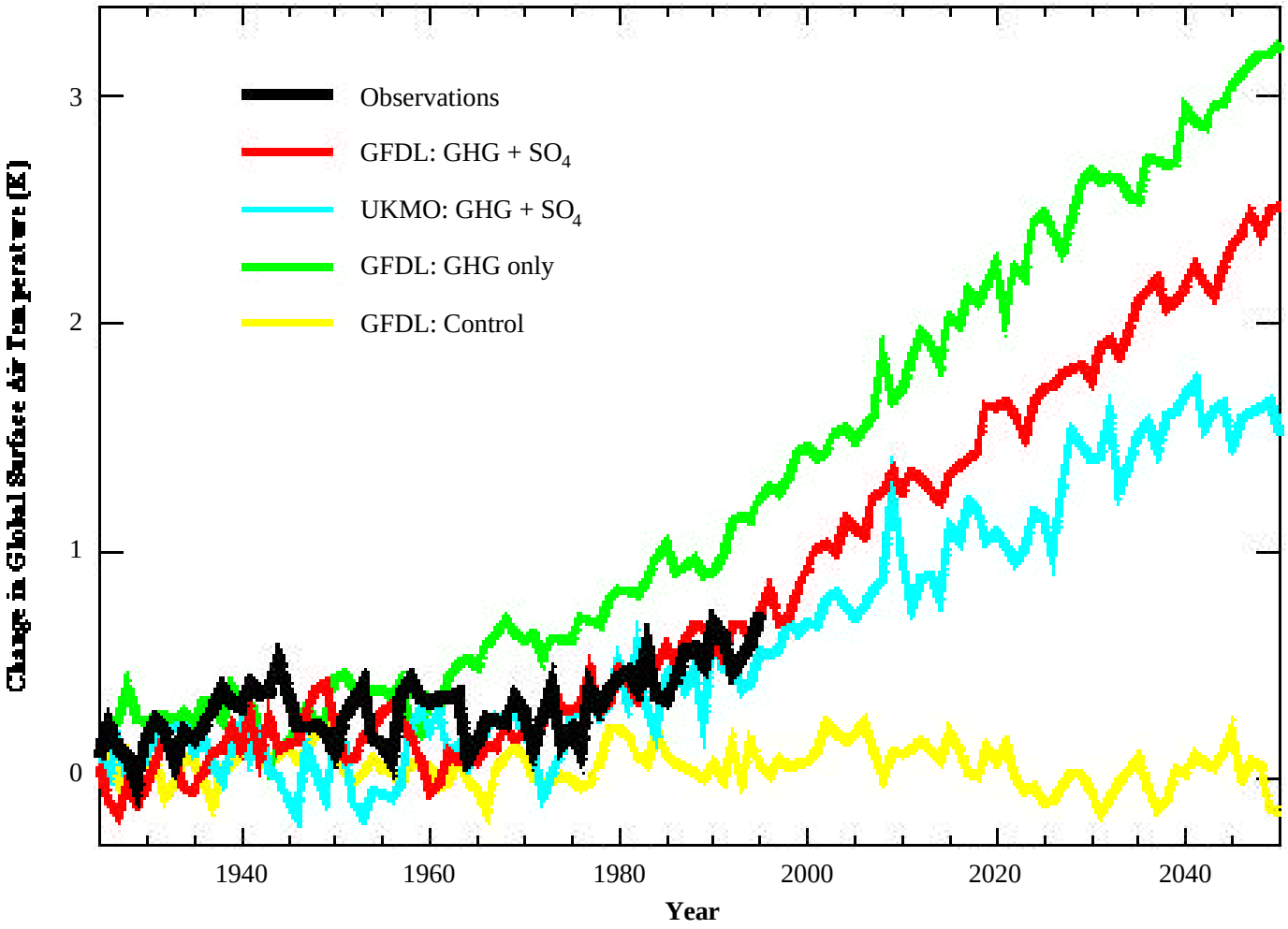

Figure 6-2: Change in global mean surface air temperature (K). Observations are from Jones (1994), modified to include data up to 1995. GFDL data are from modeling studies of Haywood *et al*. (1997b); UKMO data are from modeling studies of Mitchell *et al*. (1995).

Figure 6-1): emission of radiatively active substances (e.g., CO_2 or H_2O); emission of chemical species that produce or destroy radiatively active substances (such as NO_x, which modifies O_3 concentration, or SO_2, which oxidizes to sulfate aerosols); and emission of substances (e.g., H_2O, soot) that trigger the generation of additional clouds (e.g., contrails).

The task of detecting climate change is already difficult; the task of detecting the aircraft contribution to the overall change is more difficult because aircraft forcing is a small fraction of anthropogenic forcing as a whole. However, aircraft perturb the atmosphere in a specific way because their emissions occur in the free troposphere and lower stratosphere, and they trigger contrails, so the aircraft contribution to overall climate change may have a particular signature. At a minimum, the aircraft-induced climate change pattern would have to be significantly different from the overall climate change pattern in order to be detected.

The climatic impact of aircraft emissions is considered on the background of other anthropogenic perturbations of climate. The present assessment is based on the IS92 scenarios used to represent alternative futures in the Second Assessment Report (IPCC, 1996); it does not incorporate recent observed trends in methane (Dlugokencky *et al*., 1998), nor any implications from the Kyoto Protocol. The scenarios for aircraft flight patterns, fuel burn, and emissions are described in Chapter 9. Atmospheric perturbations are taken from detailed atmospheric models (Chapters 2, 3, and 4), except for CO_2 accumulation (which is discussed in this chapter).

The largest, single, known radiative forcing change over the past century is from the increase in CO_2, driven primarily by the burning of fossil fuel. Figure 6-3 shows the change in CO_2 over the past 1,000 years; the CO_2 concentration increased from about 280 ppmv in 1850 to about 360 ppmv in 1990. Figure 6-4 shows six IPCC projections for anthropogenic emissions of CO_2 (labeled IS92a-f) and predicted atmospheric CO_2 concentrations. We take the central case, IS92a, as the future scenario with which to compare aircraft effects. The central aircraft scenario (Fa1) assessed here matches the economic assumptions of IS92a. Radiative forcing for IS92a is shown in Figure 6-5, including total radiative forcing and individual contributions.

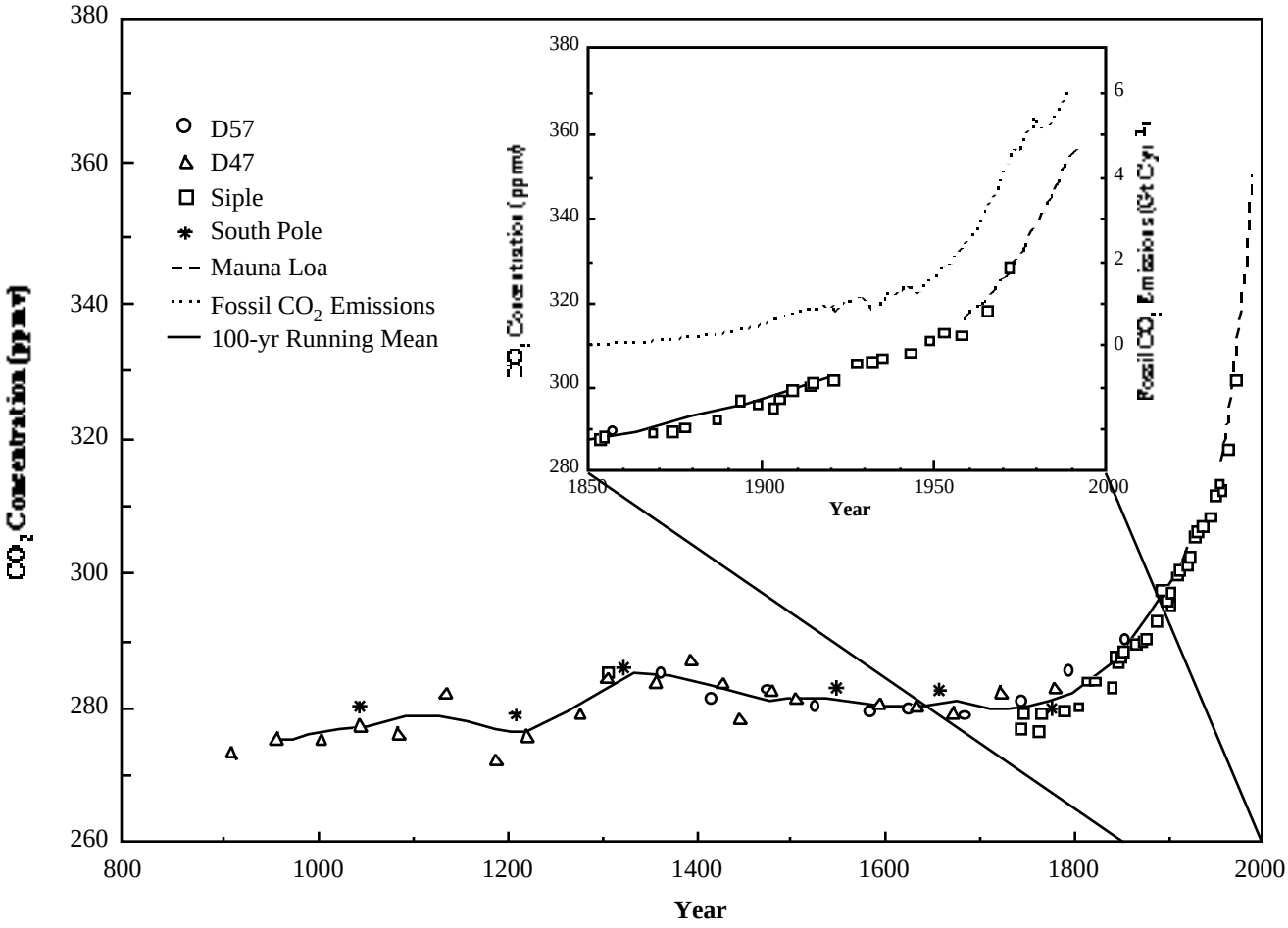

Figure 6-3: CO_2 concentration over the past 1000 years from ice core records (D47, D57, Siple, and South Pole) and (since 1958) from Mauna Loa, Hawaii, measurement site. All ice core measurements were taken in Antarctica. The smooth curve is based on a 100-yr running mean. A rapid increase in CO_2 concentration since the onset of industrialization is evident and has followed the increase in CO_2 emissions from fossil fuels (see inset for period from 1850 onward) (IPCC, 1996, Figure 1a).

6.1.3. Aviation Scenarios Adopted for Climate Assessment

A few, detailed, three-dimensional (3-D) emission inventories for three specific years—1992, 2015, and 2050—are presented in Chapter 9 and are studied with 3-D atmospheric models: NASA-1992, NASA-2015, and the ICAO-developed FESGa and FESGe scenarios for 2050. The FESG scenarios include three economic options, a/c/e, corresponding to economic growth assumed in IS92a/c/e. Each of the FESG scenarios has technology option 1 assuming typical, market-driven advances in engine/airframe technology and technology option 2 with advanced engine technology (i.e., a 25% reduction in NO_x emission index with a 3.5% increase in fuel use; see Chapter 9). Between these fixed-year scenarios, linear interpolation is used to derive continuous scenarios—Fa1, Fa2, Fc1, and Fe1 (see Table 6-3)—that extend from 1990 to 2050. CO_2 increases are derived from carbon-cycle models (see notes to Tables 6-1 and 6-2). Two scenarios based on EDF projections for the years 2015 and 2050 (Vedantham and Oppenheimer, 1998) provide only global CO_2 and NO_x emissions: the EDF-a-base (Eab) and EDF-d-high (Edh) cases. The Edh scenario was not adopted for its relationship to any underlying population or economic scenario, but because it is a smooth extrapolation of recent growth rates. Atmospheric changes other than CO_2 for Eab and Edh are scaled from the Fa1 and Fe1 scenarios (see notes to Table 6-1). The continuous scenarios are summarized in Table 6-3.

The total fuel in Gt C used by aviation from 1950 to 1992 is shown in Figure 6-6. It also shows two projections to 2050 (Fa1 and Eab; see Tables 6-1 and 6-2), comparing them with projected total fossil carbon emissions for a similar economic scenario (IS92a). Note the logarithmic scale in Figure 6-6. For scenario F1a, fuel use parallels that of IS92a, but for Eab it grows faster than total fossil fuel use. In converting aviation fuel to CO_2 emissions, we adopt a carbon fraction by weight of 86%. Aviation fuel use prior to 1992 is based on International Energy Agency data (IEA, 1991; for table, see Sausen and Schumann, 1999). To account for systematic underestimation of fuel use (see Chapter 9), we have increased NASA-1992 and NASA-2015 emissions by 15% and 5%, respectively, to form the inventories NASA-1992* and NASA-2015*. Figure 6-7 gives an expanded linear scale of aviation fuel use from 1990 to 2050 for scenarios Fc1, Fa1, Fa1H, Fe1, Eab, and Edh, in order of increasing fuel use by 2050.

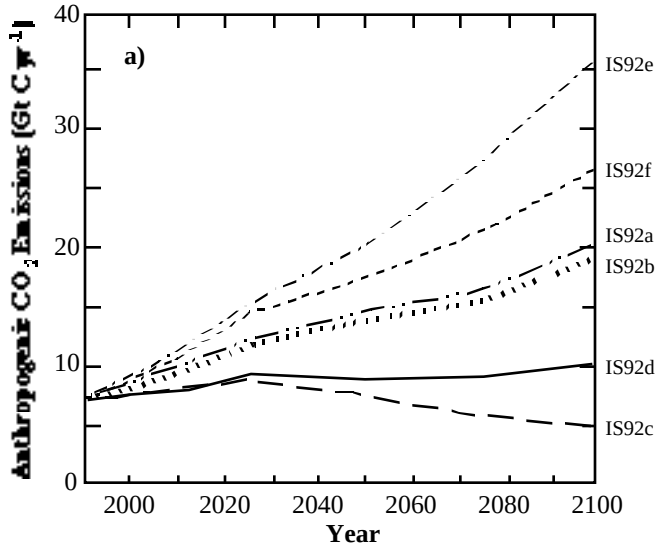

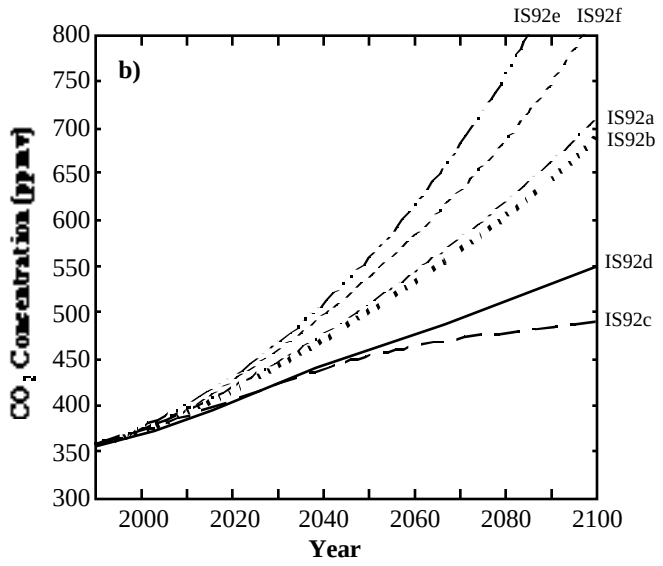

Figure 6-4: a) Total anthropogenic CO_2 emissions (Gt C yr^{-1}) under the IS92 emission scenarios, and b) the resulting atmospheric CO_2 concentrations (ppmv) calculated using the "Bern" carbon cycle model (IPCC, 1996, Figure 5).

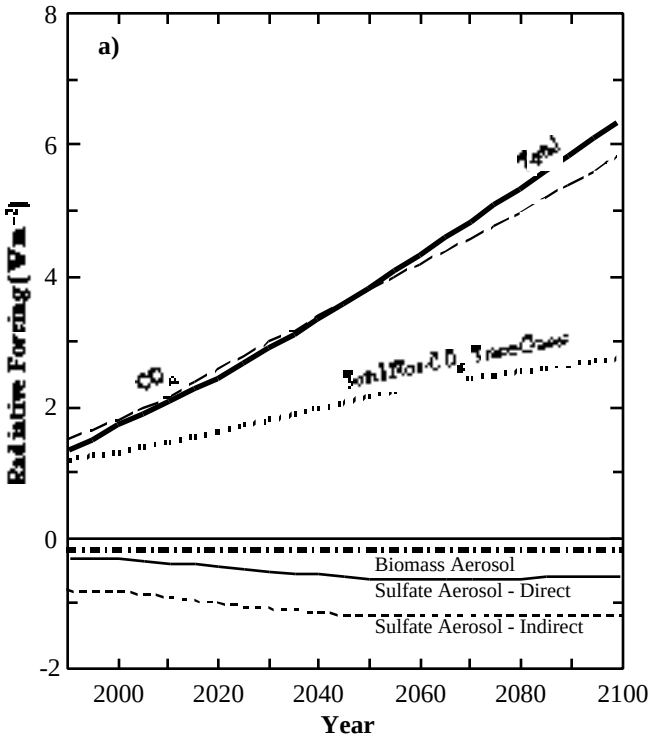

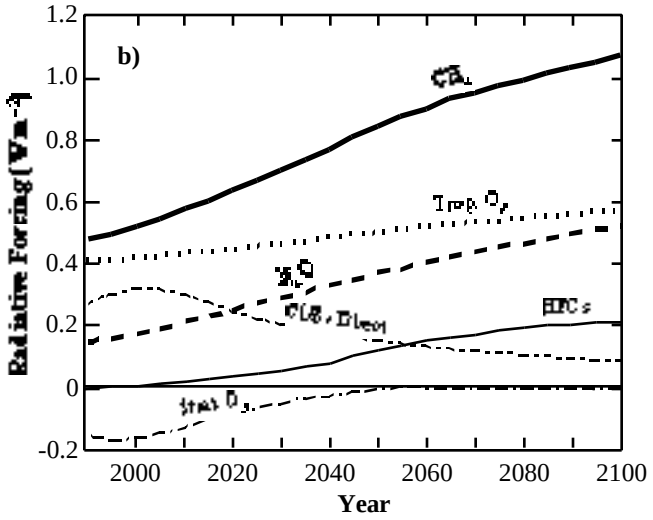

Figure 6-5: a) *Radiative forcing components resulting from the IS92a emission scenario for 1990 to 2100.* The "Total Non-CO_2 Trace Gases" curve includes the radiative forcing from CH_4 (including CH_4-related increases in stratospheric water vapor), N_2O, tropospheric O_3, and the halocarbons (including the negative forcing effect of stratospheric O_3 depletion). Halocarbon emissions have been modified to take account of the Montreal Protocol and its Adjustments and Amendments. The three aerosol components are direct sulfate, indirect sulfate, and direct biomass burning. b) *Non-CO_2 trace gas radiative forcing components.* "Cl/Br direct" is the direct radiative forcing resulting from Cl- and Br-containing halocarbons; emissions are assumed to be controlled under the Montreal Protocol and its Adjustments and Amendments. The indirect forcing from these compounds (through stratospheric O_3 depletion) is shown separately (Strat. O_3). All other emissions follow the IS92a scenario. The tropospheric O_3 forcing (Trop. O_3) takes account of concentration changes resulting only from the indirect effect from CH_4 (IPCC, 1996, Figure 6b-c).

***Table 6-1**: Aviation fixed-year (1992, 2015, and 2050) scenarios for emissions and radiative forcing.*

Scenario	Fuel Burn (Mt yr^{-1})	NO_x Emis.[d] (Mt yr^{-1})	CO_2[f] Conc. (ppmv)	Radiative Forcing (W m^{-2}) CO_2[f]	O_3[g]	CH_4[g]	H_2O[h]	Contrails[i]	Sulfate[h] Aerosols	BC[h] Aerosols	Total	RFI
NASA-1992*[a]	**160.3**	**1.92**	**1.0**	**+.018**	**+.023**	**-.014**	**+.0015**	**+.020**	**-.003**	**+.003**	**+.048**	**2.7**
Low[b]				+.013	+.011	-.005	+.000	+.005	-.001	+.001		
High				+.023	+.046	-.042	+.005	+.06	-.009	+.009		
NASA-2015*[a]	**324.0**	**4.34**	**2.5**	**+.038**	**+.040**	**-.027**	**+.003**	**+.060**	**-.006**	**+.006**	**+.114**	**3.0**
FESGa (tech1) 2050	**471.0**	**7.15**	**6.0**	**+.074**	**+.060**	**-.045**	**+.004**	**+.100**	**-.009**	**+.009**	**+.193**	**2.6**
Low				+.052	+.030	-.015	+.000	+.03	-.003	+.003		
High				+.096	+.120	-.120	+.015	+.40	-.027	+.027		
FESGa (tech2) 2050[c]	487.6	5.55	6.1	+.075	+.047	-.035	+.005	+.100	-.009	+.009	+.192	
FESGc (tech1) 2050	268.2	4.01	4.9	+.060	+.034	-.025	+.003	+.057	-.005	+.005	+.129	2.2
FESGc (tech2) 2050	277.2	3.14	5.0	+.061	+.026	-.020	+.003	+.057	-.005	+.005	+.127	
FESGe (tech1) 2050	**744.3**	**11.38**	**7.4**	**+.091**	**+.096**	**-.072**	**+.007**	**+.158**	**-.014**	**+.014**	**+.280**	**3.1**
FESGe (tech2) 2050	772.1	8.82	7.6	+.093	+.074	-.055	+.007	+.158	-.015	+.015	+.277	
EDFa-base 2015	297.0[d]	2.85	2.4	+.037	+.026	-.018	+.003	+.055	-.006	+.006	+.103	2.8
EDFa-base 2050	1143.0	7.89	9.4	+.115	+.066	-.050	+.011	+.243	-.022	+.022	+.385	3.3
EDFd-high 2015	448.0[d]	4.30	3.0	+.046	+.040	-.027	+.004	+.083	-.008	+.008	+.146	3.2
EDFd-high 2050	1688.0	11.65	13.4	+.165	+.098	-.073	+.016	+.358	-.032	+.032	+.564	3.4
HSCT (500)	**70.0**	**0.35**			**-.010**		**+.050**					
Low					-.040		+.017					
High					+.010		+.150					
HSCT (1000)	**140.0**	**0.70**			**-.010**		**+.100**					
Low					-.040		+.033					
High					+.010		+.300					
Net HSCT 2050												
+ HSCT	+140.0	+0.70	+0.8	+.010	-.010		+.100				+.100	
- subsonic	-53.6	-0.81	-0.3	-.004	-.007	+.005	-.001	-.011	+.001	-.001	-.018	
FESGa (tech1)												
+ HSCT 2050	557.4	7.04	6.5	+.080	+.043	-.040	+.103	+.089	-.008	+.008	+.275	3.4

[a] The scenarios in boldface were studied in atmospheric models with defined 3-D emission patterns; the others were scaled to these scenarios. The NASA-1992* aviation scenario has been scaled here by 1.15, and the NASA-2015* scenario by 1.05, to account for inefficiencies in flight routing.

[b] Low/High give likely (67% probability) range.

[c] In FESG scenarios, tech 1 is standard, and tech 2 reduces EI(NO_x) by 25% with a few percent additional fuel use.

[d] Throughout the table and this report, NO_x emissions (Mt yr^{-1}) and indices (EI) use the NO_2 molecular weight.

[e] In the EDF 2015 scenarios, the fuel burns have been revised to 374 (a-base) and 592 (d-high) Mt yr^{-1}, which would increase the added CO_2 by 2050 to 10.0 (a-base) and 14.7 (d-high) ppmv.

[f] CO_2 is largely cumulative and depends on the assumed previous history of the emissions; CH_4 perturbations are decadal in buildup time; all other perturbations reach steady-state balance with emissions in a few years. All except CO_2 are assumed here to be instantaneous. Thus, CO_2 concentrations are based on complete history of fuel burn—for example, scenario Fa1 = NASA-1992* → NASA-2015* → FESGa (tech1) 2050; and scenario Eab = NASA-1992* → EDFa-base 2015 → EDFa-base 2050, all with linear interpolation between 1992, 2015, and 2050 (see also Section 6.1.3).

[g] The O_3 and CH_4 RFs are scaled to NO_x emissions for non-bold scenarios.

[h] As for note g, stratospheric H_2O, sulfate, and BC aerosols scale with fuel burn.

[i] Contrails do not scale with fuel burn as the fleet and flight routes evolve (see Chapter 3). The contrail RF here is from line-shaped contrail cirrus only. Additional induced cirrus cover RF is positive, and may be of similar magnitude, but no best estimate can be given yet.

***Table 6-2**: Emissions, atmospheric concentrations, radiative forcing, and climate change (global mean surface temperature) projected for the years 1990, 2000, 2015, 2025, and 2050 using IPCC's IS92a and the aviation scenarios from Tables 6-1 and 6-3.*

	1990	2000	2015	2025	2050
Emissions					
IS92a CO_2 Emissions (Gt C yr^{-1})					
Fossil fuel	6.0	7.0	9.2	10.7	13.2
Total	7.5	8.5	10.7	12.2	14.5
Aviation CO_2 Emissions (Gt C yr^{-1})					
Fa1	0.147	0.187	0.279	0.315	0.405
Fa2	0.147	0.187	0.279	0.319	0.419
Fc1	0.147	0.187	0.279	0.265	0.231
Fe1	0.147	0.187	0.279	0.382	0.640
Eab	0.147	0.179	0.255	0.463	0.983
Edh	0.147	0.224	0.385	0.690	1.452
Fa1H	0.147	0.187	0.279	0.344	0.479
IS92a NO_x Emissions (Mt NO_2 yr^{-1})					
Energy	82	98	122	137	174
Biomass Burn	30	31	32	33	36
Aviation NO_x Emissions (Mt NO_2 yr^{-1})					
Fa1	2.0	2.8	4.3	5.1	7.2
Fa2	2.0	2.8	4.3	4.7	5.6
Fc1	2.0	2.8	4.3	4.2	4.0
Fe1	2.0	2.8	4.3	6.4	11.4
Eab	2.0	2.2	2.9	4.3	7.9
Edh	2.0	2.8	4.3	6.4	11.6
Atmospheric Concentrations					
IS92a Atmosphere					
CO_2 (ppmv)	354	372	405	432	509
CH_4 (ppbv)	1700	1810	2052	2242	2793
N_2O (ppbv)	310	319	333	344	371
Aviation Marginal CO_2 (ppmv)					
Fa1	0.9	1.5	2.5	3.5	6.0
Fa2	0.9	1.5	2.5	3.5	6.1
Fc1	0.9	1.5	2.5	3.2	4.9
Fe1	0.9	1.5	2.5	3.9	7.4
Eab	0.9	1.5	2.4	4.4	9.4
Edh	0.9	1.7	3.0	6.0	13.4
Fa1H	0.9	1.5	2.5	3.5	6.5
Aviation Marginal CH_4 (ppbv)					
Fa1	-31	-49	-75	-97	-152

Notes: The 1990 values are based on IEAdata for 1990 fuel use; these values are higher than our estimate for 1992 (see Table 6-1). The scenarios involve linear interpolation of emissions between 1990, 1992, 2015, and 2050 (see Tables 6-1 and 6-3). The projected CH_4 increases are based on the emissions growth in IS92a that do not match the much smaller trends currently observed. These calculations used the methodologies from the IPCC's Second Assessment Report (1996) as contributed by Atul Jain, Michael Prather, Robert Sausen, Ulrich Schumann, Tom Wigley, and Don Wuebbles.

Table 6-2 (continued)

	1990	2000	2015	2025	2050
Radiative Forcing					
Differential RF (W m^{-2}/ppmv)					
dRF/dCO_2	0.018	0.016	0.015	0.014	0.012
dRF/dCH_4	0.38	0.37	0.35	0.33	0.29
IS92a RF (Wm^{-2})					
CO_2	1.54	1.84	2.38	2.79	3.83
CH_4	0.47	0.51	0.59	0.66	0.83
N_2O	0.14	0.17	0.22	0.26	0.36
All greenhouse gases	2.64	3.08	3.81	4.34	5.76
Aerosols (direct and indirect)	-1.26	-1.36	-1.55	-1.66	-1.94
Total	1.38	1.72	2.26	2.68	3.82
Aviation Fa1 Components of RF (Wm^{-2})					
CO_2	0.016	0.025	0.038	0.048	0.074
O_3	0.024	0.029	0.040	0.046	0.060
CH_4	-0.015	-0.018	-0.027	-0.032	-0.045
H_2O	0.002	0.002	0.003	0.003	0.004
Contrails	0.021	0.034	0.060	0.071	0.100
Sulfate aerosol	-0.003	-0.004	-0.006	-0.007	-0.009
Soot (BC) aerosol	0.003	0.004	0.006	0.007	0.009
Indirect clouds	no best estimate available				
Total	0.048	0.071	0.114	0.137	0.193
Aviation HSCT (net) Components of RF (Wm^{-2})					
CO_2				0.001	0.006
O_3				-0.007	-0.017
CH_4				0.002	0.005
H_2O				0.040	0.099
Contrails				-0.004	-0.011
Total				0.031	0.082
Aviation Scenarios Total RF (Wm^{-2})					
Fa1	0.048	0.071	0.114	0.137	0.193
Fa2	0.048	0.071	0.114	0.136	0.192
Fc1	0.048	0.071	0.114	0.118	0.129
Fe1	0.048	0.071	0.114	0.161	0.280
Eab	0.048	0.068	0.103	0.184	0.385
Edh	0.048	0.083	0.146	0.265	0.564
Fa1H	0.048	0.071	0.114	0.168	0.275
Climate Change					
Global Mean Surface Air Temperature Change (K)					
IS92a	0.000	0.140	0.360	0.510	0.920
Fa1	0.000	0.004	0.015	0.024	0.052
Fc1	0.000	0.004	0.015	0.023	0.039
Fe1	0.000	0.004	0.015	0.026	0.070
Eab	0.000	0.004	0.014	0.026	0.090
Edh	0.000	0.005	0.019	0.038	0.133
Fa1H	0.000	0.004	0.015	0.025	0.066

***Table 6-3**: Overview of the scenarios adopted for the climate assessment.*

Name	Fixed-Year Scenario 1992	2015	2050	Comments
Fa1	NASA-1992*	NASA-2015*	FESGa	Technology option 1
Fa2	NASA-1992*	NASA-2015*	FESGa	Technology option 2
Fc1	NASA-1992*	NASA-2015*	FESGc	Technology option 1
Fe1	NASA1992*	NASA-2015*	FESGe	Technology option 1
Eab	NASA-1992*	EDF-a-base	EDF-a-base	
Edh	NASA-1992*	EDF-d-high	EDF-d-high	
Fa1H	NASA-1992*	NASA-2015*	FESGa + HSCT	Fa1 with part of subsonic traffic replaced by HSCT fleet growth from 2015 to 2040

Chapter 4 studies the impact of a fleet of high-speed civil transport (HSCT, i.e., supersonic) aircraft using a range of 3-D emission scenarios with atmospheric chemistry models. These calculations form a parametric range that covers changes in fleet size, NO_x emissions, cruise altitude, sulfate aerosol formation, and future atmospheres. The present chapter combines those results into a continuous scenario for the HSCT fleet, designated Fa1H: On top of the Fa1 scenario it assumes that HSCT aircraft come into service in 2015, grow at 40 planes per year to a final capacity of 1,000 aircraft by 2040, continue operation to 2050, and displace equivalent air traffic from the subsonic fleet (~11% of Fa1 in 2050). This Mach 2.4 HSCT fleet cruises at 18–20 km altitude and deposits most of its emissions in the stratosphere. It has new combustor technology that produces very low emissions of 5 g NO_2 per kg fuel. Table 6-1 gives the breakdown of RF from two specific HSCT studies in Chapter 4: 500 HSCTs in a 2015 background atmosphere and 1,000 HSCTs in a 2050 background atmosphere (e.g., chlorine loading, methane, nitrous oxide). The likely interval for the RF here combines the uncertainty in calculating the ozone or water vapor perturbation with that from calculating the radiative imbalance.

6.1.4. Aviation's Contribution to the CO_2 Budget

Carbon dioxide released from fossil fuel combustion rapidly equilibrates among atmosphere, surface ocean, and parts of the biosphere, leaving behind excess atmospheric CO_2 that decays slowly over the following century (see carbon cycle discussion in IPCC, 1996). Thus, for CO_2 radiative forcing, it makes no difference whether the fossil fuel is burned in aircraft or other transportation/energy sectors, and the relative role of aircraft can be found by comparing the history of fuel burned by aviation with that of total anthropogenic carbon emissions.

Comparing projected IS92a carbon emissions from fossil fuels in Figure 6-6, CO_2 emissions from aircraft in 1990 account for

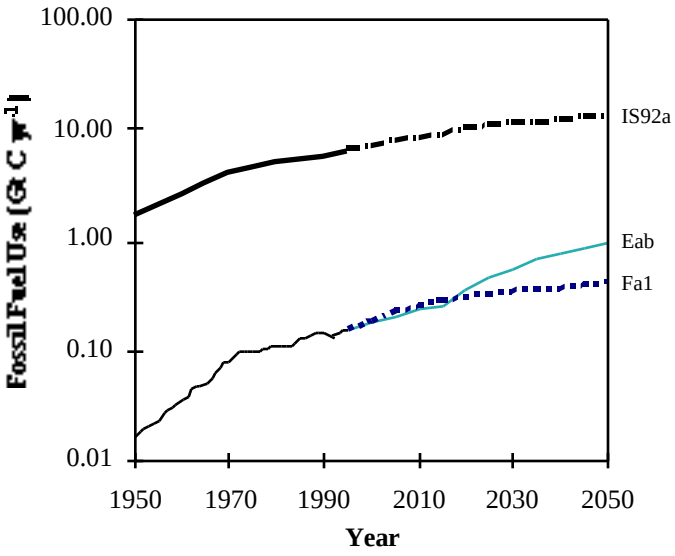

Figure 6-6: Fossil fuel use (Gt C yr^{-1}) shown for historical aviation use (1950–92, solid line) and for projected aviation scenarios Fa1 and Eab. Total historical fossil fuel use and the projection according to scenario IS92a are also shown.

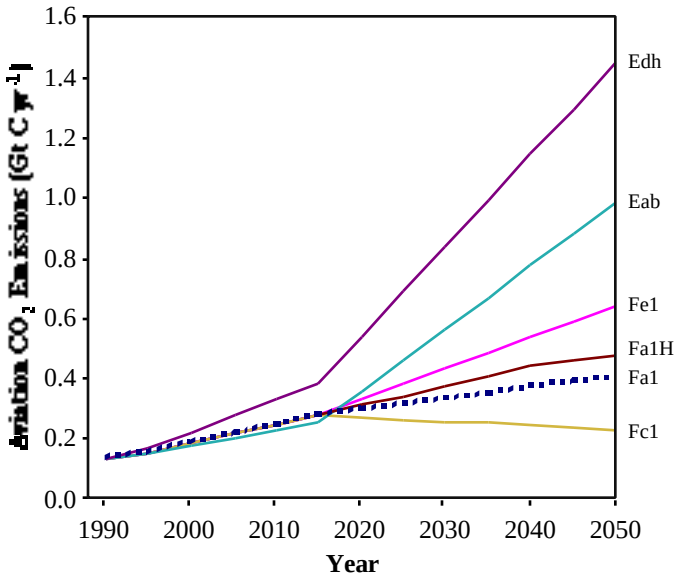

Figure 6-7: Aviation CO_2 emissions (Gt C yr^{-1}) from 1990 to 2050 for the range of scenarios considered here (see Table 6-3).

about 2.4% of the total; they are projected to grow to about 3% (Fa1) or more than 7% (Eab) of all fossil fuel carbon emissions by 2050. Sustained growth in air traffic demand (5%/yr compounded) envisaged in Edh would lead to an aviation fraction of more than 10% by 2050. By comparison, the entire transportation sector is currently about 25% of the total (see discussion in Chapter 8). Clearly, different economic projections, as well as uncertainties in predicting demand for air travel and aviation's ability to meet that demand, can alter this aviation fraction by more than a factor of 2. Technology option 2 (low-NO_x engines, Fa2) increases this fuel fraction slightly to 3.2%, and the HSCT option increases this fraction from 3.1% (Fa1) to 3.6% (scenario Fa1H, assuming no change in air traffic demand) by the year 2050.

The cumulative history of CO_2 emissions allows us to calculate the excess atmospheric CO_2 concentration attributable to aircraft, as shown in Figure 6-8. These calculations are contributed by Jain, Wigley, and Schumann using carbon cycle models consistent with IPCC (1996) and the IS92 scenarios therein. Aviation is estimated to be responsible for about 1 ppmv of the 80 ppmv rise in CO_2 from 1860 to 1990. Uncertainty in the prediction of atmospheric CO_2 is estimated to be ±25%. Resulting CO_2 radiative forcing is only one part of aviation's climate impact. Other changes in greenhouse gases, radiatively important aerosols, and clouds—as noted in Figure 6-1 and broken out in Table 6-1—must be included. The remaining sections of this chapter examine aviation's total role in climate change over the next 50 years for the example scenarios given in Table 6-3.

6.2. Radiative Forcing and GWP Concepts

6.2.1. The Concept of Radiative Forcing

The most useful assessment of the impact of the aircraft fleet on climate would be a comprehensive prediction of changes to the climate system, including temperature, sea level, frequency of severe weather, and so forth. Such assessment is difficult to achieve given the current state of climate models and the small global forcing of climate attributable to the single sector of aviation chosen for this special report (see discussion in Sections 6.1 and 6.5). Following IPCC (1995, 1996), we choose a single measure of climate change: radiative forcing (RF), which is calculated directly from changes in greenhouse gases, aerosols, and clouds, and which allows ready comparison of the climate impact of different aviation scenarios.

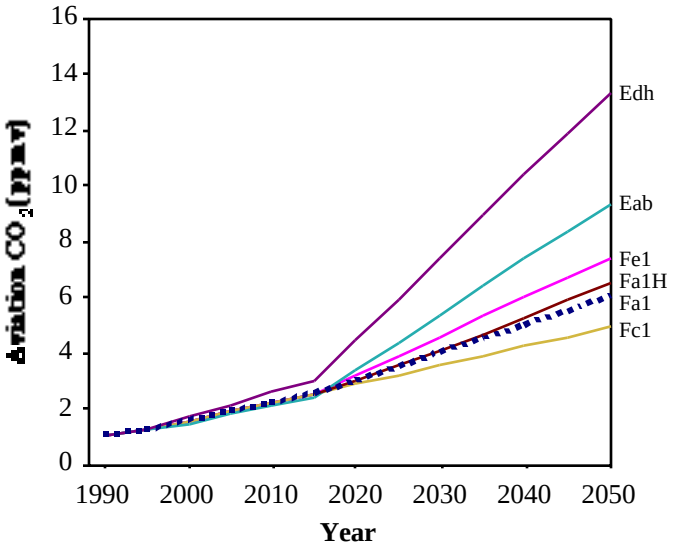

Figure 6-8: Atmospheric CO_2 (ppmv) accumulated from aviation's use of fossil fuel beginning in 1940.

The Earth's climate system is powered by the sun. Our planet intercepts 340 W m^{-2} of solar radiation averaged over the surface of the globe. About 100 W m^{-2} is reflected to space, and the remainder—about 240 W m^{-2}—heats the planet. On a global average, the Earth maintains a radiative balance between this solar heating and the cooling from terrestrial infrared radiation that escapes to space. When a particular human activity alters greenhouse gases, particles, or land albedo, such activity results in radiative imbalance. Such an imbalance cannot be maintained for long, and the climate system—primarily the temperature and clouds of the lower atmosphere—adjusts to restore radiative balance. We calculate the global, annual average of radiative imbalance (W m^{-2}) to the atmosphere-land-ocean system caused by anthropogenic perturbations and designate that change radiative forcing. Thus, by this IPCC definition, the RF of the pre-industrial atmosphere is taken to be zero. (Although the term "radiative forcing" has more general meaning in terms of climate, we restrict its use here to the IPCC definition.)

As an example, burning of fossil fuel adds the greenhouse gas CO_2 to the atmosphere; this burning is responsible for the increase in atmospheric CO_2 from about 280 ppmv in the pre-industrial atmosphere to about 360 ppmv in 1995. Added CO_2 increases the infrared opaqueness of the atmosphere, thereby reducing terrestrial cooling with little impact on solar heating. Thus, the radiative imbalance created by adding a greenhouse gas is a positive RF. Apositive RF leads to warming of the lower atmosphere in order to increase the terrestrial radiation and restore radiative balance. Radiative imbalances can also occur naturally, as in the case of the massive perturbation to stratospheric aerosols caused by Mt. Pinatubo (Hansen *et al*., 1996).

Because most of the troposphere is coupled to the surface through convection, climate models typically predict that the land surface, ocean mixed layer, and troposphere together respond to positive RF in general with a relatively uniform increase in temperature. Global mean surface temperature is a first-order measure of what we consider to be "climate," and its change is roughly proportional to RF. The increase in mean surface temperature per unit RF is termed climate sensitivity; it includes feedbacks within the climate system, such as changes in tropospheric water vapor and clouds in a warmer climate. The RF providing the best metric of climate change is the radiative imbalance of this land-ocean-troposphere climate system—that is, the RF integrated at the tropopause.

When radiative perturbation occurs above the tropopause, in the stratosphere (as for most HSCTimpacts), this heating/cooling is not rapidly transported into the troposphere, and the imbalance leads mostly to changes in local temperatures that restore the radiative balance within the stratosphere. Such changes in stratospheric temperature, however, alter the tropospheric cooling; for example, warmer stratospheric temperatures lead to a warmer troposphere and climate system. This adjustment of stratospheric temperatures can be an important factor in calculating RF and is denoted "stratosphere-adjusted."

All RF values used in this report refer to "stratosphere-adjusted, tropopause RF" (*Shine et al.*, 1995). For primarily tropospheric perturbations (e.g., CO_2 from all aviation, O_3 from subsonic aircraft), this quantity can be calculated with reasonable agreement (better than 25%) across models used in this report (see Section 6.3). For specifically stratospheric perturbations (e.g., H_2O and O_3 perturbations from HSCT aircraft), the definition of the tropopause and the calculation of stratospheric adjustment introduce significant sources of uncertainty in calculated RF.

The concept of radiative forcing (IPCC, 1990, 1992, 1995) is based on climate model calculations that show that there is an approximately linear relationship between global-mean RF at the tropopause and the change in equilibrium global mean surface (air) temperature (ΔT_s). In mapping RF to climate change, the complexities of regional and even hemispheric climate change have been compressed into a single quantity—global mean surface temperature. It is clear from climate studies that the climate does not change uniformly: Some regions warm or cool more than others. Furthermore, mean temperature does not provide information about aspects of climate change such as floods, droughts, and severe storms that cause the most damage. In the case of aviation, the radiative imbalance driven by perturbations to contrails, O_3, and stratospheric H_2O occurs predominantly in northern mid-latitudes and is not globally homogeneously distributed (see Chapters 2, 3, and 4), unlike perturbations driven by increases in CO_2 or decreases in CH_4. Does this large north-south gradient in the radiative imbalance lead to climate change of a different nature than for well-mixed gases? IPCC (Kattenberg *et al.*, 1996) considered the issue of whether negative RF from fossil-fuel sulfate aerosols (concentrated in industrial regions) would partly cancel positive RF from increases in CO_2 (global). Studies generally confirmed that global mean surface warming from both perturbations was additive; that is, it could be estimated from the summed RF. Local RF from sulfate in northern industrial regions was felt globally. Nevertheless, the regional patterns in both cases were significantly different, and obvious cooling (in a globally warming climate) occurred in specific regions of the Northern Hemisphere. Such differences in climate change patterns are critical to the detection of anthropogenic climate change, as reported in Santer *et al*. (1996). As a further complication of this assessment, aviation's perturbation occurs primarily in the upper troposphere and lower stratosphere, and thus may alter the vertical profile of any future tropospheric warming. Therefore, the patterns of climate change from individual aviation perturbations (e.g., CO_2, O_3, contrails) would likely differ, but we take their summed RF as a first-order measure of the global mean climate change (see also the discussion in Section 6.5).

The equilibrium change in mean surface air temperature ($\Delta T_s^{(equil)}$) in response to any particular RF is reached only after more than a century because of the thermal inertia of the climate system (primarily the oceans) and is calculated with long-term integrations of coupled general circulation models (CGCM). A climate sensitivity parameter (λ) relates *RF* to temperature change: $\Delta T_s^{(equil)} = \lambda\, RF$. Provided that all types of RF produce the same impact on the climate system (in this case measured by mean temperature), the climate sensitivity parameter derived from a doubled-CO_2 calculation can be used to translate other RFs, say from ozone or contrails, into a change in global mean surface air temperature.

For doubled CO_2 relative to pre-industrial conditions (+4 Wm^{-2}), surface temperature warming ranges from 1.5 to 4.5 K, depending on the modeling of feedback processes included in the CGCM. The recommended value in IPCC (1996) of 2.5 K gives a climate sensitivity of λ = 0.6 K/(W m^{-2}). With limited feedbacks (e.g., fixing clouds and surface ocean temperatures), the sensitivity parameter is smaller, and most models produce similar responses. In contrast, when all feedbacks are included, model results are quite different, as a result (for instance) of alternative formulation of clouds. The obvious limitation of this approach is that we get no information about regional climate change. The sensitivity parameter for aircraft-like ozone perturbations is discussed in Section 6.5.

In spite of all these caveats, the radiative forcing of an aviation-induced atmospheric perturbation is still a useful index that allows, to first approximation, the different atmospheric perturbations (e.g., aerosols, cloud changes, ozone, stratospheric water, methane) to be summed and compared in terms of global climate impact.

6.2.2. Global Warming Potential

Global warming potential (GWP; see Shine *et al*., 1990, for a formal definition) is an index that attempts to integrate the overall climate impacts of a specific action (e.g., emissions of CH_4, NO_x or aerosols). It relates the impact of emissions of a gas to that of emission of an equivalent mass of CO_2. The duration of the perturbation is included by integrating radiative forcing over a time horizon (e.g., standard horizons for IPCC have been 20, 100, and 500 years). The time horizon thus includes the cumulative climate change and the decay of the perturbation.

GWP has provided a convenient measure for policymakers to compare the relative climate impacts of two different emissions. However, the basic definition of GWP has flaws that make its use questionable, in particular, for aircraft emissions. For example, impacts such as contrails may not be directly related

to emissions of a particular greenhouse gas. Also, indirect RF from O_3 produced by NO_x emissions is not linearly proportional to the amount of NO_x emitted but depends also on location and season. Essentially, the buildup and radiative impact of short-lived gases and aerosols will depend on the location and even the timing of their emissions. Furthermore, the GWP does not account for an evolving atmosphere wherein the RF from a 1-ppm increase in CO_2 is larger today than in 2050 and the efficiency of NO_x at producing tropospheric O_3 depends on concurrent pollution of the troposphere.

In summary, GWPs were meant to compare emissions of long-lived, well-mixed gases such as CO_2, CH_4, N_2O, and hydrofluorocarbons (HFC) for the current atmosphere; they are not adequate to describe the climate impacts of aviation.

Nevertheless, some researchers have calculated a GWP, or modified version, for aircraft NO_x emissions via induced ozone perturbation (e.g., Michaelis, 1993; Fuglestvedt *et al*., 1996; Johnson and Derwent, 1996; Wuebbles, 1996). The results vary widely as a result of model differences, varying scenarios for NO_x emission, and the ambiguous GWP definition for short-lived gases. There is a basic impossibility of defining a GWP for "aircraft NO_x" because emissions during takeoff and landing would have one GWP; those at cruise, another; those in polar winter, another; and those in the upper tropical troposphere, yet another. Different chemical regimes will produce different amounts of ozone for the same injection of NO_x, and the radiative forcing of that ozone perturbation will vary by location (Fuglesvedt *et al.*, 1999). In view of all these problems, we will not attempt to derive GWPindices for aircraft emissions in this study. The history of radiative forcing, calculated for the changing atmosphere, is a far better index of anthropogenic climate change from different gases and aerosols than is GWP.

6.2.3. Alternative Indexing of Aviation's Climate Impact—RF Index

A new alternative index to measure the role of aviation in climate change is introduced here: the radiative forcing index (RFI), which is defined as the ratio of total radiative forcing to that from CO_2 emissions alone. Total radiative forcing induced by aircraft is the sum of all forcings, including direct emissions (e.g., CO_2, soot) and indirect atmospheric responses (e.g., CH_4, O_3, sulfate, contrails). RFI is a measure of the importance of aircraft-induced climate change other than that from the release of fossil carbon alone. RFI ranges between 2.2 and 3.4 for the various E- and F-type scenarios for subsonic aviation and technical options considered here (see Section 6.6). Thus, aircraft-induced climate change with RFI > 1 highlights the need for a thorough climate assessment of this sector as performed here. For comparison, in the IS92a scenario the RFI for all human activities is about 1; for greenhouse gases alone, it is about 1.5, and it is even higher for sectors that emit CH_4 and N_2O without significant fossil fuel use.

6.3. Radiative Forcing from Aircraft-Induced Changes in Greenhouse Gases

This section presents RF calculations for perturbations to greenhouse gases attributable to aircraft. Greenhouse gases that have been identified as aircraft-perturbed are CO_2, O_3, CH_4, and H_2O. Each gas presents a special case in terms of predicting its perturbation or deriving radiative forcing. The RF calculations presented here are derived from radiative-balance and comprehensive climate models by subtracting net radiative flux (incoming solar minus outgoing terrestrial infrared) for a control run from that for a run that includes the specified perturbation. In general, these calculations integrate over a full range of latitudinal and seasonal variations that are typical of the Earth's climate, consider the imbalance at the tropopause, and account for the adjustment of stratospheric temperatures. Important factors in deriving representative radiative forcing include realistic temperatures, water vapor, surface albedo, clouds, and tropopause. RF calculations represent the instantaneous imbalance in the troposphere-land-ocean system, thus do not include responses that are considered part of the climate feedback system, such as changes to clouds and tropospheric water vapor.

RF values depend on atmospheric composition as well as temperature, water vapor, and clouds because all of these factors interact with the radiation field. For these calculations, we have adopted the changing composition as specified in IS92a from IPCC (1995) and summarized in Table 6-2. This composition includes substantial increases in CO_2 and CH_4 that alter the Earth's radiation spectrum, thus change the RF for a given unit increase of gas. Although we expect mean global warming of about 1 K by 2050, with concurrent changes in water vapor and possibly cloud cover, there is no consensus in IPCC (1996) regarding what this future atmosphere would be. Thus, these RF values for 2050 are not based on a future climate, and this discrepancy must add to the uncertainty of this assessment. However, all such potential, systematic errors apply equally to the baseline scenario IS92a, and the relative climatic impact of aircraft will have less uncertainty.

6.3.1. Models for Radiative Forcing

Calculation of radiative forcing from 3-D models is a relatively new endeavor. The history of this calculation began with one-dimensional models (e.g., Hansen *et al*., 1984a) that made use of the basic radiative-convective model approach initiated by Manabe and Wetherald (1967). Subsequent researchers expanded this calculation, using GCM output to describe atmospheric lapse rate, water vapor, and cloud cover and including latitudinal and seasonal changes (e.g., Pollack *et al.* 1993). Both the radiative perturbations from aircraft and the background radiative constituents (e.g., clouds, water vapor, albedo) vary with altitude, latitude, longitude, and time.

Three-dimensional modeling of radiative forcing introduces substantial complexity. The different modeling groups cited

here have different approaches to calculating RF, involving choices in spatial and temporal domains.

All models report instantaneous values of radiative forcing at the top of the atmosphere and at the tropopause; in other words, these RF values have been calculated with no changes in atmospheric temperature. As discussed in Section 6.2.1, the most appropriate RF value includes allowance for stratospheric temperatures to readjust to radiative perturbation. Only two groups (Forster and Haywood, and Ponater and Sausen—see paragraphs below) have models that allow for such stratospheric adjustment. This correct, adjusted RF usually lies between the instantaneous values at the top of the atmosphere and the tropopause, and we correct the RF reported from other groups so that all RF values here refer to tropopause radiative forcing with stratospheric adjustment.

RF modeling results were contributed by P. Forster and J. Haywood (Forster and Shine, 1997), A. Grossman (Grossman *et al*., 1997), J. Haywood (Haywood and Ramaswamy, 1998), D. Rind (Rind and Lonergan, 1995), W.-C. Wang (Wang *et al.*, 1995), and M. Ponater and R. Sausen (Ponater *et al*., 1998).

Forster and Haywood's radiation scheme has been previously used to calculate ozone and water vapor radiative forcings; it is described in Forster and Shine (1997). It employs a 10 cm^{-1} narrowband model (Shine, 1991) in the thermal infrared (IR) and a discrete-ordinate model (Stamnes *et al*., 1988) at solar wavelengths with 5-nm resolution in the ultraviolet (UV) and 10-nm resolution in the visible. As in Forster and Shine (1997), the fixed dynamic heating approximation (Ramanathan and Dickinson, 1979) is used to calculate stratospheric temperature perturbations. A zonally and annually averaged, 5° latitudinal resolution climatology was used as the basis for the forcing calculations. Temperature and humidity were derived largely from European Centre for Medium-range Weather Forecasts (ECMWF) analyses, averaged over the period 1980–91. In the upper stratosphere, temperatures were derived from Fleming *et al*. (1990). At pressures less than 300 hPA, humidity was based on a combination of Stratospheric Aerosol and Gas Experiment II (SAGE-II) and Halogen Occultation Experiment (HALOE) data. Surface albedos, cloud amounts, and optical depths were 7-year averages from International Satellite Cloud Climatology Project (ISCCP) (Rossow and Schiffer, 1991). Clouds were specified at three levels. The thermal infrared calculations included absorption by nitrous oxide, methane, and carbon dioxide. Ozone climatologies were taken from an observed climatology derived by Li and Shine (1995), a combination of SAGE-II, Solar Backscatter Ultraviolet (SBUV), Total Ozone Mapping Spectometer (TOMS), and ozonesonde data. To calculate forcing, the climatological profiles were perturbed by the absolute annual averages of ozone and water vapor changes.

Grossman (Grossman *et al*., 1997) uses a set of baseline annual and longitudinal average atmospheric profiles, resolved by 50 layers between 0 and 60 km, at latitudes of 60°N/S, 30°N/S, and at the Equator that are scaled to IS92A (IPCC, 1995) composition. Supersonic and subsonic aircraft O_3 and H_2O perturbation profiles were added to the baseline atmospheric profiles for RF calculations. The Lawrence Livermore National Laboratory (LLNL) 16-band solar radiation model (Grant and Grossman, 1998) and the LLNL 32-band IR radiation model (Chou and Suarez, 1994) were used to calculate instantaneous tropopause and top-of-atmosphere RFs at each latitude for the global average value for O_3 and H_2O.

Haywood's RF calculations for sulfate and black carbon aerosols were made following the method of Haywood and Ramaswamy (1998). The Geophysical Fluid Dynamics Laboratory (GFDL) R30 GCM incorporates a 26 band delta-Eddington solar radiative code (Ramaswamy and Freidenreich, 1997) and includes the cloud parameterization of Slingo (1989) and aerosol optical properties calculated using Mie theory. RF calculations are performed at the top of the atmosphere every day using mean solar zenith angle. No account is made for stratospheric adjustment, the effects of which are likely to be small for tropospheric aerosol in the solar spectrum.

Ponater and Sausen estimated instantaneous RF using the ECHAM4 GCM (Roeckner *et al*., 1996). Radiative transfer calculations (one radiative time step only) were performed for each grid point with and without local ozone perturbation, including the actual cloud profile. Several diurnal cycles were calculated for each calendar month, and the radiative flux change was determined for each individual grid point at the top of the atmosphere and at the tropopause. The annual global mean radiative forcing was obtained by averaging over all grid points and over the seasonal cycle. To calculate the stratosphere-adjusted, tropopause RF, a "second atmosphere" was implemented into the ECHAM4 GCM. Whereas the primary atmosphere of the GCM does not "feel" the perturbation of the greenhouse gas, the second atmosphere experiences an additional radiative heating above the tropopause, although dynamic heating is identical to that of the first, unperturbed atmosphere. In the troposphere, the primary and second atmospheres are not allowed to diverge. In this configuration, the model is run for one annual cycle.

Rind used the Goddard Institute for Space Studies (GISS) Global Climate Middle Atmosphere Model (Rind *et al*., 1988). The radiation scheme in the model is the correlated-k method for modeling non-gray gaseous absorption (Lacis and Oinas, 1991). The procedure involved keeping re-start files and full diagnostics for the first full day of each month from a control run. Radiation and all other routines were called each hour, so a full, diurnal average global response was calculated. Then the first day of each month was re-run with altered atmospheric composition (e.g., changes in ozone). The global net radiation at the top of the atmosphere was compared. The assumption is that with only 1 day of running time, temperatures would not adjust (even in the stratosphere) to the altered composition; hence, the results are instantaneous values.

Wang's RF calculations use the National Center for Atmospheric Research (NCAR) Community Climate Model 3 (CCM3) radiative model with monthly mean, latitude-by-longitude

distributions of vertical temperature, moisture, clouds, and surface albedo simulated from the Atmospheric Model Intercomparison Project (AMIP). The year 1992 of the CCM3-AMIP simulations was used because the corresponding year was used to simulate ozone in the Oslo 3-D CTM (Isaksen *et al*., 1999). Because this State University of New York/ Albany version of CCM3 used the ozone climatology (Wang *et al*., 1995), CTM-simulated absolute ozone changes for 1992–2015 and 1992–2050 are mapped onto 1992 ozone climatology to calculate the RF. RFs are based on fixed temperature treatment rather than fixed dynamic heating treatment (Wang *et al*., 1993).

6.3.2. Radiative Forcing for CO_2

Carbon dioxide has a long atmospheric residence time (on the order of many decades); hence, aircraft CO_2 becomes well mixed within the atmosphere and can be treated together with other anthropogenic CO_2 emissions in conventional global warming simulations (e.g., Washington and Meehl, 1989; Cubasch *et al*., 1992; Murphy and Mitchell, 1995). The aircraft influence depends on the temporal evolution of the amount of the CO_2 increase that can be attributed to aircraft emissions, which is directly proportional to the amount of fuel burned. See Section 6.1.2 and Table 6-2 for the calculation of CO_2 increases attributed to aviation.

Over the period 1990 to 2050, under IS92a we expect an increase in atmospheric CO_2 of about 155 ppmv from burning of fossil fuels, cement production, and other anthropogenic activities that release biospheric carbon. By 2050, F-type aviation scenarios produce a 5–7 ppmv increase, and the high-growth Edh scenario leads to a 13 ppmv increase. Thus, aviation in these scenarios would be responsible for 3–8% of the total anthropogenic increase in CO_2 from 1990 to 2050.

The RF for aviation CO_2 in 1992 is estimated to be +0.018 Wm^{-2}, with a likely range of ±30% that includes uncertainties in the carbon cycle and in radiative calculations (see WMO, 1999). Uncertainties and confidence intervals discussed here do not include possible errors in predicting future scenarios. By 2050, the different aviation scenarios have a range of +0.06 to +0.16 W m^{-2}. The technology option 2 scenario (Fa2) leads to a 0.1 ppmv increase in CO_2 by 2050, with only a small increase in CO_2-RF.

The HSCToption, F1aH, has 18% greater fuel use but only 8% greater CO_2 concentrations by 2050, with a corresponding increase in CO_2-RF from +0.074 to +0.080 W m^{-2}. Because the HSCT fleet has just reached maturity in 2040, the extra fuel consumption of the HSCT aircraft is barely felt in terms of the accumulation of CO_2. Similarly, the CO_2 impact of new subsonic technologies that are introduced linearly between 2015 and 2050 is not fully effected by 2050. A fuller evaluation would have to extend the assessment beyond 2050, when the cumulative effects of mature fleets would be felt (e.g., Sausen and Schumann, 1999).

6.3.3. Radiative Forcing for O_3

Ozone is a potent greenhouse gas whose concentration is highly variable and controlled by atmospheric chemistry and dynamics. Aircraft emissions of NO_x accelerate local photochemical production of O_3 in the troposphere; modeling studies suggest that these emissions are responsible today for average O_3 enhancements of 2–5 ppbv in the middle troposphere at northern mid-latitudes, where most aircraft fly (see Chapters 2 and 4). This ozone increase will generally be proportional to the amount of NO_x emitted (Grewe *et al*., 1999), but evolving atmospheric composition, including increases in surface sources of combustion-related NO_x, will affect the aircraft impact.

Four subsonic ozone perturbations based on detailed 3-D patterns of NO_x emissions were chosen (along with their control atmospheres) for the calculation of RFs: NASA-1992, NASA-2015, FESGa (tech 1), and FESGe (tech 1) at 2050. Results for NASA-1992 were scaled by 1.15 to give NASA-1992*, and those for NASA-2015 by 1.05 to give NASA-2015*. Table 6-1 describes some of the basic properties of these aircraft scenarios, including total NO_x emissions. Chapter 4 supplied the seasonal pattern of O_3 perturbations for these scenarios based on model calculations and reported a factor of 2 uncertainty in this best value. The modeled RFs from these O_3 perturbations agree quite well, and the stratospheric temperature adjustment does not greatly affect the result (as was confirmed by two independent model calculations). Given the predominantly tropospheric perturbation, the uncertainty in modeling RF is small, and the uncertainty in the final result may be a factor of only 3. The ozone RFs are +0.023 W m^{-2} for NASA-1992*, +0.040 W m^{-2} for NASA-2015*, and +0.060 W m^{-2} for FESGa (tech1) 2050 (see also Table 6-1).

The development of atmospheric chemistry models in the past 2 years has allowed a consensus to build such that aircraft ozone perturbations can be calculated with a likely (2/3 probability) range of about a factor of 2 (higher/lower, see Chapter 4). Our estimate of the resulting RF for this predominantly tropospheric perturbation does not significantly enhance that interval.

The NASA-1992, NASA-2015, and FESGa (tech 1) at 2050 scenarios produce global mean column ozone increases (predominantly tropospheric) of 0.5, 1.1, and 1.7 Dobson Units (DU), respectively. Our estimate of the increase in tropospheric ozone associated with all anthropogenic changes (IS92a including aircraft plus surface emissions of NO_x, CO, and hydrocarbons) is about 3 DU from 1992 to 2015 and 7 DU from 1992 to 2050. These results represent an advance in our understanding since the Second Assessment Report (IPCC, 1996), when future ozone changes were scaled only to CH_4 increases and did not include the effects of doubling NO_x emissions from 1990 to 2050.

Two HSCT cases with detailed 3-D emission scenarios—one with 500 aircraft and the other with 1,000 aircraft—were used to calculate RF from stratospheric O_3 and H_2O perturbations (see Table 6-1). Most of the ozone change occurs above the

tropopause; thus, there is poorer agreement among RF models and a greater difference in RF values after stratospheric temperatures adjust. The ozone perturbation calculated for 500 supersonic aircraft with the 2015 background atmosphere is substantially different in nature from that calculated for 1,000 aircraft with the 2050 atmosphere, in part because of specified changes in chlorine and methane contents of the stratosphere (see Chapter 4). Nevertheless, the best RF values are about the same: -0.01 W m^{-2}. The uncertainty range in these values is large and changes sign (-0.04 to +0.01 W m^{-2}), reflecting not only the range in O_3 perturbations given by Chapter 4 but also the large uncertainty in deriving RF for stratospheric perturbations. This ozone-related RF for the HSCT fleet is based only on the stratospheric ozone perturbation calculated by the models in Chapter 4; the tropospheric changes are discarded, and a correction for the displacement of about 11% of the subsonic traffic is included, as shown in Table 6-1 (scenario Fa1H).

6.3.4. Radiative Forcing for CH_4

Methane is a long-lived, well-mixed greenhouse gas. It has an atmospheric lifetime of about 9 years. The tropospheric chemical models used to evaluate the impact of the subsonic fleet found unanimously that CH_4 lifetime was reduced by aircraft emissions (see Chapter 4). This instantaneous change (-1.3% in 1992, -2.6% in 2015, and -3.9% in 2050 for scenario FSEGa (tech1)) needs to be increased further by a factor of 1.4 to include the feedback of CH_4 concentrations on lifetime (Prather, 1994; IPCC, 1996). It is then applied to the IS92a CH_4 abundance to calculate the reduction in CH_4 concentration that can be attributed to aircraft. The CH_4 perturbation is assumed to be instantaneous; in reality, however, it takes a couple of decades to appear and will lag the O_3 perturbation. For the purposes of interpolating between RF points in Table 6-1, we assume that the CH_4 perturbation, like the O_3 perturbation, is proportional to NO_x emissions.

6.3.5. Radiative Forcing for H_2O

Water vapor is a potent greenhouse gas that is highly variable in the troposphere, with a short average residence time controlled by the hydrological cycle. In the stratosphere, the slow turnover of air and extreme dryness make precipitation and clouds a rare phenomena, leading to smoothly varying concentrations ranging from 3 to 6 ppmv as CH_4 is oxidized to H_2O (Dessler *et al.*, 1994; Harries *et al.*, 1996). The contribution of aircraft to atmospheric H_2O is directly from the H in the fuel (assumed to be 14% by mass). Most of the subsonic fleet's fuel is burned in the troposphere, where this additional source of water is swamped by the hydrological cycle. A smaller fraction is released in the stratosphere, where longer residence times may lead to greater accumulation. However, because flight routes are close to the tropopause and reach at most into the lowermost stratosphere, this effluent is rapidly returned to the troposphere with little expected accumulation (Holton *et al.*, 1995; see also Section 3.3.4).

Although the uncertainty of predicting the current subsonic RF for water vapor is large—a factor of 3—the absolute number in 1992 is estimated to be sufficiently small, +0.0015 W m^{-2}, making this factor a minor uncertainty in subsonic climate forcing. It is assumed that this value scales linearly with fuel use (see Table 6-1). This value is consistent with earlier studies: Schumann (1994) and Fortuin *et al.* (1995) estimated that present air traffic enhances background H_2O by less than 1.5% for regions most frequently used by aircraft; likewise, Ponater *et al.* (1996) and Rind *et al.* (1996) used GCM studies to conclude that the direct radiative effect on the climate of water vapor emissions from 1992 air traffic is negligibly small.

The projected HSCT fleet, however, would cruise at 20-km altitude and build up much greater H_2O enhancements in the stratosphere. The stratospheric models described in Chapter 4 predicted excess stratospheric water vapor from an HSCT fleet of 500 aircraft (designated HSCT(500) in Table 6-1). This perturbation is difficult to calculate, and the likely (2/3 probability) range includes a factor of 2 higher and lower. Furthermore, RF modeling of this stratospheric H_2O perturbation adds further uncertainty, as indicated in Table 6-1. All results suggest that this effect is the dominant HSCT climate impact, with RF equal to +0.05 (0.017 to 0.15) W m^{-2} for 500 aircraft, increasing to +0.10 (0.03 to 0.30) W m^{-2} for a mature fleet of 1,000 aircraft (HSCT(1000)). Although it takes several years to accumulate this excess stratospheric water vapor, it is assumed that this RF is instantaneously proportional to the HSCT fleet size.

In a GCM study, Rind and Lonergan (1995) looked for climate change caused by H_2O accumulation from a fleet of 500 HSCTs. They found no statistically significant change in surface temperature. Their result is consistent with this assessment and with water vapor as the dominant HSCT climate impact because the magnitude of this radiative forcing from the fleet, +0.05 W m^{-2}, would induce a mean global warming that would be difficult to detect above natural climate variability.

6.3.6. Uncertainties

Assignment of formal uncertainty—or the likely (2/3 probability) interval about the best value—to radiative forcing caused by aircraft perturbations is difficult. For well-mixed gases (e.g., CO_2, CH_4) or for well-defined tropospheric perturbations (subsonic O_3), there is small uncertainty in calculated RF. In these cases, the overall uncertainty interval lies with calculating the perturbation itself: 25% for CO_2, a factor of 2 for O_3, and a factor of 3 for CH_4. For perturbations to stratospheric ozone and water, there is much greater uncertainty in calculating RF, especially because in these cases radiative forcing at the tropopause can be substantially different after stratospheric temperatures adjust. In addition, HSCT-induced ozone and water vapor perturbations—with large variations in the lower stratosphere—present a much more difficult calculation of RF where the placement of the modeled tropopause can lead to additional uncertainty.

As an example of the uncertainty in calculating RF values from an adopted ozone perturbation, the NASA-1992 tropospheric ozone perturbation was calculated by several groups, as shown in Table 6-4. The instantaneous RF at the tropopause is consistent across the models, and the stratospheric adjustment (calculated by two groups) is consistently 0.001 to 0.002 W m^{-2} less. For the HSCT(500) water vapor perturbation, the two groups have significantly greater disagreement, and the correction following stratospheric adjustment is a large fraction of tropopause instantaneous RF. This water vapor perturbation is the result of averaging six model results, and an additional RF is calculated using the water vapor perturbation calculated with a 3-D model that lies at the lower end of this ensemble (Grossman*; see Table 6-4). This table highlights the robustness of calculated RF for tropospheric perturbations and the much greater uncertainty in deriving climate forcing for stratospheric changes.

Uncertainty ranges about the best values are given in Table 6-1 for the NASA-1992* and FESGa (tech 1) 2050 subsonic scenarios and for some components of supersonic scenarios HSCT(500) and HSCT(1000). These intervals are intended to represent the same probability range (67% likelihood), but there is no uniform statistical model (e.g., Gaussian) for all of them, nor are the individual RF contributions fully independent; hence, these ranges cannot be combined into a confidence interval on total RF.

6.4. Radiative Forcing from Aircraft-Induced Changes in Aerosols and Cloudiness

There are two mechanisms by which aerosols may exert radiative forcing: the direct effect, whereby aerosol particles scatter and absorb solar and longwave radiation; and the indirect effect, whereby aerosol particles act as cloud condensation nuclei and modify the physical and radiative properties of clouds. Additionally for aircraft, merely flying through certain meteorological environments can result in formation of contrails (Section 3.4), which affect both solar and longwave radiation budgets. The present-day direct radiative forcing from aircraft emissions of sulfur compounds and black carbon aerosols is investigated in Sections 6.4.1 and 6.4.2; radiative forcing from the formation of contrails and the indirect effect of aerosol emissions is investigated in Section 6.4.3. Section 6.4.4 derives future RF considering our range of scenarios for fuel use. The RF models have been described previously (Section 6.3.1). A summary of radiative forcing calculations and related uncertainties is given in Section 6.4.5.

6.4.1. Direct Radiative Forcing from Sulfate Aerosols

Sulfate aerosol scatters a fraction of incident solar radiation back to space, thereby leading to negative direct radiative forcing. The direct radiative forcing of pure sulfate in the longwave spectrum is likely to be negligible as a result of the size of aerosol particles and the corresponding wavelength dependence of the specific extinction coefficient (e.g., Haywood and Shine, 1997; Haywood *et al*., 1997a). Myhre *et al*. (1998) summarize 10 detailed studies of the sensitivity of direct radiative forcing from all anthropogenic sources of sulfate. With the exception of one study, sensitivities per unit column mass of anthropogenic sulfate range from -125 to -214 W g^{-1} SO_4.

We reexamined these results by inserting a pure ammonium sulfate in a layer between 8 and 13 km in the GFDLR30 GCM and assuming an ambient relative humidity of 45% using the method of Haywood and Ramaswamy (1998). A log-normal

***Table 6-4**: Results of RF (W m^{-2}) for the 1992 aviation-induced ozone perturbation and for the water vapor from the HSCT(500) fleet as calculated by several models (see section 6.3.1).*

NASA-1992 Tropospheric Ozone Perturbation

Type of RF Calculation	*Forster & Haywood*	*Ponater & Sausen*	*Grossman*	*Rind*	*Wang*
Top of atmosphere, instantaneous	+0.014	+0.021	+0.013	+0.011	+0.010
Tropopause, instantaneous	+0.020	+0.026	+0.022		+0.020
Tropopause, after stratospheric adjustment	+0.019	+0.024			

HSCT(500) Stratospheric Water Vapor Perturbation

Type of RF Calculation	*Forster & Haywood*	*Ponater & Sausen*	*Grossman*	*Grossman**
Top of atmosphere, instantaneous	+0.001	+0.001	-0.002	-0.001
Tropopause, instantaneous	+0.096	+0.049	+0.074	+0.048
Tropopause, after stratospheric adjustment	+0.068	+0.034		

*RF calculation for a lower accumulation rate of H_2O (Danilin *et al*., 1998; Hannegan *et al*., 1998).

distribution with a dry geometric mean radius of 0.05 µm and a standard deviation of 2.0 was adopted. The resulting global mean sensitivity was found to be approximately -215 Wg^{-1} SO_4, which is adopted throughout this report. Because the modeled pure sulfate particles scatter incident radiation with no absorption, the RF is not sensitive to their location relative to the tropopause. Thus, the RF is well approximated by the instantaneous radiative forcing at the top of the atmosphere even for aircraft sulfate in the lower stratosphere.

Astudy of the distribution of aircraft fuel burned and transported as a passive tracer from scenario NASA-1992 involved a range of global models and is presented in Chapter 3 (see also Danilin *et al*., 1998). The median global mean column burden of sulfate aerosol is derived in this study by adopting an emission index for sulfur EI(S) of 0.4 g kg^{-1} and a 50% effective conversion factor from fuel-sulfur to optically active sulfate aerosols; it is approximately 13.5 µg SO_4 m^{-2} (Table 3-4). Thus, global mean radiative forcing from aircraft emissions of sulfate aerosol in 1992 is estimated to be -0.003 W m^{-2}, with a likely range of -0.001 to -0.009 W m^{-2} (see also Table 6-1). This value is much smaller in absolute magnitude than the RF from CO_2, O_3, CH_4, or contrails. We assume that EI(S) remains constant through 2050 and scale the sulfate RF with fuel use.

6.4.2. Direct Radiative Forcing from Black Carbon Aerosols

Tropospheric black carbon (BC) aerosol, also described as soot, primarily absorbs incident solar radiation, which leads to positive radiative forcing. As in the case of sulfate aerosol, the small size of the particles means that radiative forcing in the longwave region of the spectrum is likely to be negligible. The sensitivity of global mean radiative forcing to column loading of total anthropogenic BC is estimated by Haywood *et al*. (1997a), Haywood and Ramaswamy (1998), and Myhre *et al*. (1998) to range from approximately +1100 to +1850 W g^{-1} BC.

We reexamined results by inserting BC aerosol in a layer between 8 and 13 km in the GFDLR30 GCM using the method of Haywood and Ramaswamy (1998). Alog-normal distribution with a geometric mean radius of 0.0118 µm and a standard deviation of 2.0 was assumed. The resulting global mean sensitivity was found to be approximately +3000 W g^{-1} BC as a result of the higher sensitivity of the radiative forcing when the BC exists at higher altitudes above a greater proportion of cloudy layers (Haywood and Ramaswamy, 1998). This value is adopted throughout this report because it explicitly takes into account the effect of the elevated altitude of the aerosol.

BC particles primarily absorb sunlight and heat the local air. Thus, unlike BC that resides in the troposphere, BC in the stratosphere contributes negative solar radiative forcing that is countered by induced positive longwave radiative forcing. Thus, radiative forcing from BC aerosols is sensitive to their location relative to the tropopause. We do not have enough information on the location of BC relative to the tropopause, and thus our use of the instantaneous top-of-atmosphere value overestimates the RF depending on the fraction of aircraft BC in the lower stratosphere.

Using the aircraft fuel-burn scenarios for NASA-1992 noted above and described in Chapter 3, we derive a global mean column burden of BC aerosol from aircraft of 1.0 µg BC m^{-2} (assuming an EI(BC) of 0.04 g kg^{-1}; see also Table 3-4). Thus, we estimate global mean BC aerosol forcing in 1992 to be +0.003 (+0.001 to +0.006) W m^{-2} and assume that it linearly scales with fuel use (see also Table 6-1). This value is much smaller in absolute magnitude than the RF from CO_2, O_3, CH_4, or contrails.

6.4.3. Radiative Forcing from Persistent Contrails and Indirect Effects on Clouds

Aircraft emission of water vapor and particles, as well as the creation of contrails, could lead to a change in global cloudiness. Some atmospheric GCM studies that have looked at the impacts of injecting water vapor or creating contrails (e.g., Ponater *et al*., 1996; Rind *et al*. 1996) point to the potential importance of these effects on climate, but these pilot studies cannot be used directly in this assessment. Persistent contrails clearly related to aircraft are detectable, however, and their impact on radiative forcing can be evaluated. Section 3.6 (see Table 3-9) estimates direct radiative forcing from persistent contrails to be +0.02 (+0.005 to +0.06) W m^{-2} in 1992 (see also Table 6-1). This estimate is limited to immediately visible, quasi-linear persistent contrails.

Whereas contrail formation and associated radiative forcing is an obvious and visible consequence of aircraft activity, the secondary, indirect effect of aerosols from aircraft on the microphysical and radiative properties of clouds is a very complex issue that has received little attention and is very difficult to quantify (Seinfeld, 1998). Some significant steps in quantifying the indirect effect from anthropogenic aerosols have been made (e.g., Jones *et al*., 1994; Boucher and Lohmann, 1995). The effects of aerosol particles from aircraft emissions on clouds are more complicated because nucleation and subsequent growth of ice crystals that make up cirrus clouds are more complex and less studied than for water clouds. Cirrus cloud generally exert positive forcing because longwave positive radiative forcing is of a larger magnitude than solar negative radiative forcing. Section 3.6.5 (see Table 3-9) estimates that radiative forcing from aircraft-induced cirrus is positive and may be comparable to contrail RF. The magnitude of this RF remains very uncertain. No best estimate is given in Tables 6-1 and 6-2, but a range for the best estimate could fall between 0 and 0.04 W m^{-2}.

6.4.4. Future Scenarios

Direct RF from sulfate and BC in the future is obtained by scaling the best values for 1992 to future fuel use (see Table 6-1). By 2050, it is projected to increase by factors of about 2–5 for F-type

scenarios and 7–10 for E-type scenarios. Atmospheric levels of aircraft sulfate and BC are assumed to respond instantaneously to fuel burn. RF values for these future scenarios given in Table 6-1. For the central FESGa (tech1) 2050 scenario, RF(sulfate) is estimated to be -0.009 (-0.003 to -0.027) W m^{-2}, and RF(BC) is estimated to be +0.009 (+0.003 to +0.027) Wm^{-2}. The magnitude of radiative forcing for sulfate and BC aerosol from subsonic aircraft appears to cancel, but this appearance is deceptive because EI(S) and EI(BC) are highly uncertain for the future fleet and are not coupled. For the range of scenarios listed in Table 6-1, each of these RFs remains smaller than the RF from CO_2, O_3, or persistent contrails; these effects still need to be considered, however, especially in the upper limits of the uncertainty range.

We do not evaluate here the climate impact of sulfate and BC aerosols from the projected HSCT fleet (scenario Fa1H). Sulfate released near 20 km would augment the natural Junge layer, adding about 25% to total mass and a smaller fraction to reflectivity (see discussion in Chapter 4). These numbers depend on the sulfur content of HSCT fuel. BC aerosols released from HSCT aircraft would primarily heat the stratosphere and may lead to a small negative value of RF after stratospheric adjustment. Still, the EI(S) and EI(BC) from yet-to-be-developed HSCT aircraft are highly uncertain but are likely to be much smaller than other HSCT-induced RF.

If RF from contrails of +0.02 W m^{-2} in 1992 (see Section 3.6) scales with fuel burn, it would increase to +0.06 W m^{-2} by the year 2050 (Fa1). However, contrails are expected to increase more rapidly than global aviation fuel consumption as a consequence of a number a factors: Air traffic is expected to increase mainly in the upper troposphere, where contrails form preferentially; newer, more efficient engine/airframes will travel greater distances with the same amount of fuel, but larger wide-body aircraft carry more passengers and burn more fuel for the same distance; and more efficient aircraft can trigger contrails at higher atmospheric temperatures, hence at a larger range of altitudes (see discussion in Section 3.7 and Gierens *et al*., 1999). Thus, global mean RF for persistent contrails is predicted to be larger by an additional factor of 1.6 (+0.10 Wm^{-2}). Technology option 2 (scenario Fa2) does not increase contrail RF because the same distances are flown although the fuel burned is greater.

The radiative forcing from aircraft-induced cirrus clouds in 2050 is even more uncertain than for 1992 (Chapter 3). An estimate could fall between 0 and 0.16 Wm^{-2} for the 2050 FESGa (tech1) scenario.

Persistent contrails in the stratosphere are not likely because of the low ambient relative humidity. Radiative forcing from contrails from the proposed HSCT fleet may therefore be neglected in future scenarios of radiative forcing (except for the 11% reduction of subsonic RF from air traffic displaced by HSCT aircraft).

6.4.5. Uncertainties

It is difficult to constrain the direct and indirect climate effects of aerosols from aircraft. Measurements at altitude are not adequate to define the aircraft contribution today, so models representing emissions and subsequent chemical and physical transformations have adopted differing parameterizations to estimate atmospheric concentrations. Furthermore, different aerosol size distributions, the hygroscopic nature of some of the aerosol constituents, and mixing of different species of aerosol all lead to uncertainties in the radiative properties of aerosols. These uncertainties in the burden and radiative properties of aerosols emitted by aircraft lead to associated uncertainties in radiative forcing that are much larger than for a well-mixed, directly emitted greenhouse gas such as carbon dioxide.

RF from aircraft emissions of greenhouse gases and aerosols can be constrained when the amount of radiatively important species is directly limited by emissions (e.g., CO_2, H_2O, sulfate, BC). However, it is more difficult to place upper limits on RF when the climate impact occurs indirectly, as in aircraft NO_x production of O_3 or—specifically here—in perturbations to naturally occurring clouds by aircraft aerosols.

The indirect effect of aerosols from aircraft emissions on naturally occurring clouds cannot be quantified at present owing to the complexity of several processes such as ice-cloud nucleation and the dependence of albedo and emissivity on the size of the ice crystals. With our present knowledge, this uncertainty must be considered significant. Radiative forcing from contrails is estimated to grow disproportionately with fuel use, and extrapolation to large values in 2050 is an important uncertainty in the future radiative impact of aviation. Further uncertainty arises from the fact that all estimates of contrail RF were made for the present climate, hence do not account for future climate change (see discussion in Section 3.7.1).

6.5. Relation between Radiative Forcing and Climate Change

6.5.1. Radiative Forcing and Limits of the Concept

In Sections 6.3 and 6.4 we have reported radiative forcing calculations for various aspects of aircraft-induced perturbations to radiatively active substances. One of the basic ideas behind this calculation was the validity of the concept of RF as a quantitative predictor for climate change (see Section 6.2.1). We implicitly assume that contributions from individual perturbations to the change in global mean surface temperature are additive, at least as a first-order approximation. The radiative forcing concept requires a quasi-constant climate sensitivity parameter λ within the same model for different types of RF and different magnitudes of RF. This assumption holds for changes in most of the well-mixed greenhouse gases and for variations in solar irradiance (e.g., Hansen *et al.*, 1984b; Shine *et al*., 1995; Hansen *et al*., 1997b; Roeckner *et al*., 1999). As noted in previous IPCC reports (e.g., IPCC, 1996), there are limitations to the applicability of the radiative forcing concept, especially for RFs that are highly variable geographically or seasonally (i.e., typical of aircraft perturbations).

As a clear example of large spatial differences in radiative forcing, the annual mean radiative imbalance as a function of

latitude is shown in Figure 6-9 for the big four RFs for subsonic aviation in 1992. Whereas the radiative imbalances from CO_2 (positive) and CH_4 (negative) are nearly uniform from south pole to north pole, those from O_3 (peaking at 0.065 W m^{-2} at 30°N) and contrails (peaking at 0.10 W m^{-2} at 40°N) are highly concentrated in northern mid-latitudes. The global means of all four contributions are about equal (see Table 6-1). The NO_x-driven perturbations to O_3 and CH_4 produce RFs (+0.23 and -0.14 W m^{-2}, respectively) that are of similar magnitude and in part cancel. However, the latitudinal distribution of the radiative imbalance from these two perturbations does not cancel: The combined O_3+CH_4 forcing is positive in the Northern Hemisphere and negative in the Southern Hemisphere. The response of the climate system to such geographically non-homogeneous forcing is unknown. At least regional differences in climate response can be expected, and there may even be differences in the global mean response (see Section 6.5.2).

The limitations and advantages of the radiative forcing concept have recently been demonstrated by Hansen *et al.* (1997b). A classic test case considers radiative forcing and associated climate change for ozone perturbations occurring at different altitudes. In a series of numerical experiments with a low-resolution GCM (Hansen *et al.*, 1997a), the impact of 100 DU ozone added to the various model layers was investigated. As in the calculations of Lacis *et al.* (1990), Hauglustaine and Granier (1995), Forster and Shine (1997), and Brasseur *et al*. (1998), strong variation of radiative forcing with the altitude of ozone perturbation is found: negative forcing for perturbation in the middle stratosphere, and positive forcing for perturbation in the troposphere and lower stratosphere. RF is a maximum for a perturbation close to the tropopause (Figure 6-10, dotted curve).

Without cloud and water vapor feedbacks, the change in global-mean surface air temperature exhibits a similar dependency on the altitude of the ozone perturbation as radiative forcing does (with a maximum close to the tropopause, not shown in figure). However, when all model feedbacks are included, the maximum global-mean surface temperature change in the GISS model occurs for an ozone perturbation in the middle troposphere (Figure 6-10, dashed line). The climate sensitivity parameter λ varies widely as a function of the altitude of the ozone perturbation varies widely from the middle stratosphere to the surface layer (Figure 6-10, solid line). Peak sensitivity in this model occurs in the lower troposphere because of feedbacks on clouds. However, for the altitude range at which aircraft O_3 perturbations contribute significantly to the total RF (e.g., 2–14 km), the value of λ is within a factor of 2 of the climate sensitivity parameter for doubling of CO_2 in the same model, 0.92 K/(W m^{-2}) (Hansen *et al.*, 1997b).

In GCM experiments with a similar model that focused on aircraft-like perturbations, the specific feedbacks that minimized the response for aircraft releases were high-level cloud cover (Rind and Lonergan, 1995—considering ozone impacts) and

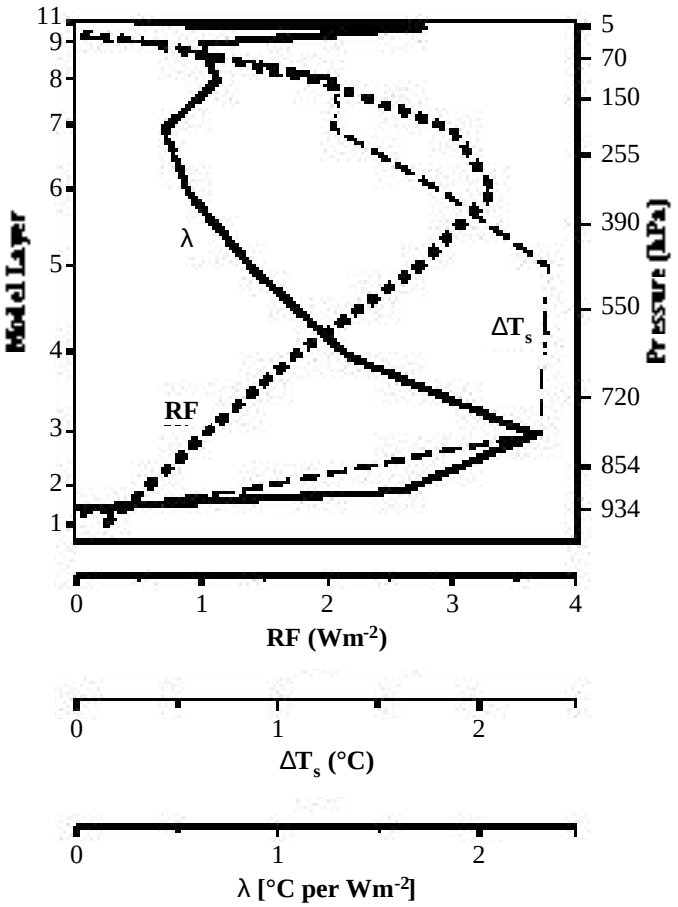

Figure 6-10: Radiative forcing (dotted line), global mean surface temperature change including all internal feedback processes (dashed line), and climate sensitivity parameter λ (solid line) from 100 DU additional ozone as a function of altitude (model layer) to which ozone was added. The plot is based on results of a simplified GCM (data from Table 3 by Hansen *et al*., 1997b).

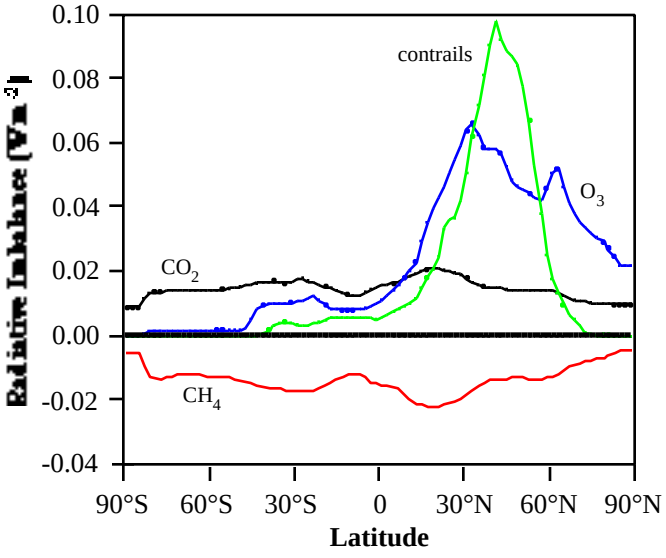

Figure 6-9: Zonal and annual mean radiative imbalance (Wm^{-2}) at the tropopause (after adjustment of stratospheric temperature) as a function of latitude as a result of air traffic for 1992.

sea ice (Rind *et al*., 1996—considering water vapor releases). Sensitivity of λ to layered perturbations is also found by Ponater *et al.* (1998) but with opposite sense: The climate sensitivity parameter for aircraft-induced ozone is *higher* than that for well-mixed greenhouse gases. The difference in these results likely depends on the formulation of clouds within the two models.

With our present understanding of climate modeling and critical feedback processes in the troposphere, we can do no better than adopt the tropopause value of RF after stratospheric adjustment. However, for aircraft-induced climate perturbations, the additivity of RFs across all perturbations cannot be taken for granted and adds further uncertainty.

6.5.2. Climate Signatures of Aircraft-Induced Ozone Perturbations

With uncertainty in relating RF to climate response noted above, it would be useful to compare CGCM-modeled climate responses for aircraft perturbations. Less agreement is expected between models because the magnitude of their feedback responses (i.e., climate sensitivity) can be quite different from one another. A review of different model sensitivities has been given in IPCC (1990, 1992, 1996); the values vary from a sensitivity of about 0.4 K/(Wm^{-2}) to 1.2 K/(Wm^{-2}) for doubled CO_2. How the sensitivity would vary for heterogeneous aircraft perturbations is not known.

The most appropriate tool would be simulations in the transient mode using coupled atmosphere-ocean GCMs. These simulations are computationally very expensive, and it would be very difficult to separate signal from noise. To date, however, all known comprehensive model simulations of aircraft-induced climate change were made in the quasi-stationary mode using either pure atmospheric GCMs (e.g., Sausen *et al.*, 1997) or atmospheric GCMs coupled to mixed layer ocean models (examples below). In other words, these simulations studied quasi-equilibrium response to a stationary or seasonally repeating perturbation. Pure atmospheric models underestimate the response if, for instance, sea surface temperature is fixed to a prescribed value. Equilibrium simulations with coupled models overestimate the aircraft effect in absolute numbers relative to transient simulations (see discussion in Sausen and Schumann, 1999), and the spatial pattern of climate change can serve only as a first estimate (Kattenberg *et al.*, 1996). These simulations must be compared with analogous simulations for well-mixed greenhouse gases (e.g., CO_2 doubling). Then the particular climate sensitivity to aircraft-induced radiative forcing and aircraft signatures of climate changes may possibly be extracted.

Using the GISS 3-D climate/middle atmosphere model, Rind and Lonergan (1995) studied the impact of the combined effect of a stratospheric ozone decrease and a tropospheric ozone increase from an assumed sub- and supersonic aircraft fleet for the year 2015. An equilibrium climate simulation leads to a general stratospheric cooling of a few tenths of a Kelvin, combined with a warming of the lower stratosphere in northern polar regions as a result of altered atmospheric circulation (Figure 6-11). The globally averaged surface temperature change was found to be not statistically significant compared with climatic variability.

As another example, Figure 6-12 shows the equilibrium annual, zonal mean temperature change from ECHAM4/MLO (Ponater *et al*., 1998) due to ozone perturbations resulting from 1992 air traffic (Dameris *et al.*, 1998), which differ slightly from the 1992 ozone perturbations reported in this assessment. The overall pattern of temperature change is statistically significant. The RF associated with this case is 0.04Wm^{-2}, and the resulting equilibrium change of global mean surface temperature is 0.06 K, resulting in a climate sensitivity parameter λ of about 1.5 K/(W m^{-2}). Note that a climate sensitivity calculated for such small perturbations is associated with large uncertainty.

For comparison, Figure 6-13 shows the equilibrium climate change associated with the anthropogenic increase of well-mixed greenhouse gases (CO_2, CH_4, etc.) from 1990 to 2015 according to IS92a as simulated with the same model. The associated global mean surface temperature change is 0.9 K, and the RF is 1.1 W m^{-2}. The resulting climate sensitivity parameter, about 0.8 K/(W m^{-2}), is smaller than for the aircraft-induced ozone perturbation. Temperature change patterns are quite different for well-mixed greenhouse gases than for the aircraft-induced ozone perturbation.

These and related experiments with the GISS and ECHAM4 models showed that: The aircraft-related climate change pattern and the aircraft-related climate sensitivity parameters are model-dependent, and the climate response for aircraft-induced ozone changes is different from that for conventional greenhouse gases. Internal feedback processes within and between climate models appear to work differently. The exact nature of the climate feedback differences to different pattern of RF remains to be investigated. Thus, the climate factors of human interest, especially the regional climate change for these regional perturbations, await further development of climate models. The details of the climate response to the contrail radiative imbalance, which is spatially heterogeneous on the smallest scales, is likewise unknown.

6.6. The Role of Aircraft in Climate Change—Evaluation of Sample Scenarios

The overall impact of aviation on climate change in the next 50 years is evaluated here for a range of scenarios (see Section 6.1.3 and Table 6-3) in air traffic and potential options in civil aviation (e.g., low-NO_x combustors, high-speed civil transport). Aviation's role is considered within the context of climate change already being forced by greenhouse gases and expected to continue from growth of the world's economies (e.g., IPCC's IS92a scenario; see IPCC, 1992). The impact of air travel and climate change as a whole on society is beyond this scientific assessment of the role of aviation in physical climate change.

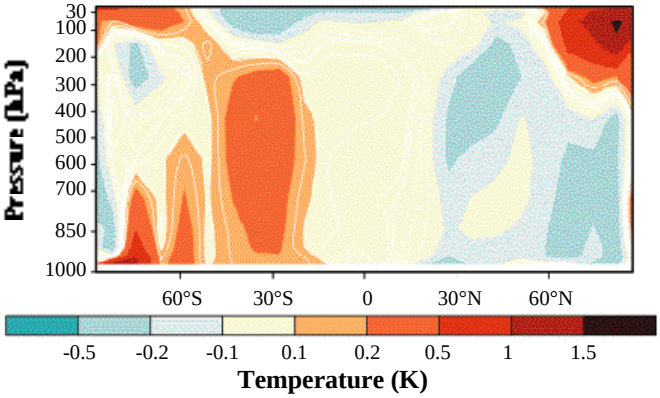

Figure 6-11: Equilibrium change of annual, zonal mean temperature (K) caused by ozone perturbation due to NO_x emissions of a projected sub- and supersonic aircraft fleet for the year 2015, as simulated with the GISS model (Rind and Lonergan, 1995). This calculation is not for any specific scenarios assessed here.

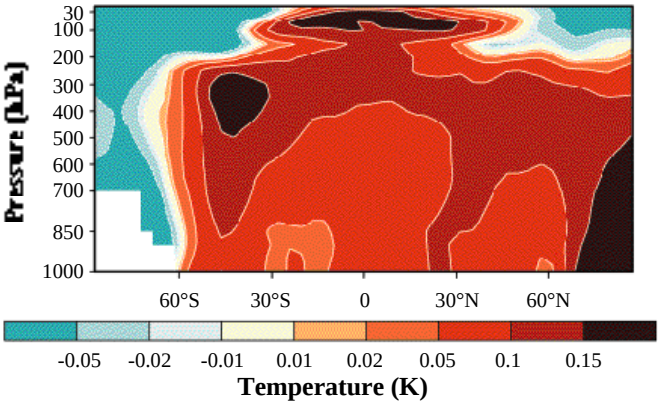

Figure 6-12: Equilibrium change of annual, zonal mean temperature (K) caused by ozone perturbation due to NO_x emissions of 1991–92 air traffic (DLR-2), as simulated with the ECHAM4/MLO model (Ponater *et al*., 1998). This result is similar to, but not based on, the scenarios analyzed here.

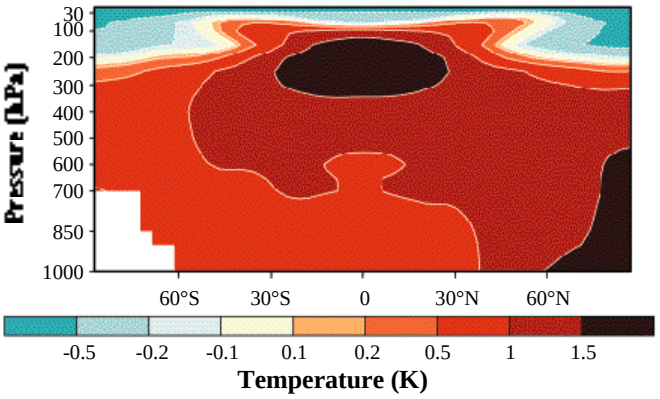

Figure 6-13: Equilibrium change of annual, zonal mean temperature (K) resulting from the anthropogenic increase of well-mixed greenhouse gases from 1990 to 2015, as simulated with the ECHAM4/MLO model (Ponater *et al*., 1998).

This section combines the aviation impacts from Sections 6.3 and 6.4 evaluated for the fixed-year scenarios (defined in Table 6-1) and places them in a continuous time sequence (defined in Table 6-3) to compare with overall climate changes expected under IS92a. We assume that RFs are additive, so the issue of different climate sensitivities—for example, for aircraft-induced ozone perturbations versus those from CO_2 (as discussed in Section 6.5)—introduces some additional error/ uncertainty when we use summed RF to deduce climate change. We have no alternative but to use RF as a metric of climate change because differences in forcing between the various subsonic options would not be reliably detected above the natural climate variability in many models. The summed RF, however, should provide a relative ranking of the different options discussed below.

6.6.1. Individual Components of Radiative Forcing

Figure 6-14a (IPCC, 1996) shows a bar chart of individual components of RF for all anthropogenic change for the 1990 atmosphere. This figure can be compared with 1992 aircraft RF components from the NASA-1992* scenario in Figure 6-14b (note the change of scale; see also Table 6-1). Aircraft RF is qualitatively different from overall anthropogenic RF: The CH_4 RF is negative, the O_3-RF is greater than the CO_2-RF, and the aerosol-cloud effects are positive (because of persistent contrails) rather than negative. Within the error bars, the effects of CO_2, O_3, and contrails are comparable; that of methane is also comparable, but negative. A caveat here is that we are unable to derive a best estimate for the indirect effects from aircraft on "natural" clouds; these effects might be negligible or may be comparable to that of contrails. Thus, for 1992 our best estimate is that aviation causes RF (without additional cirrus) of approximately +0.05 W m^{-2} and is responsible for about 3.5% of the total anthropogenic RF of about +1.4 W m^{-2} for greenhouse gases plus aerosols (+2.7 W m^{-2} for greenhouse gases alone).

Bar charts for the 2050 atmosphere are presented in Figure 6-15. The same qualitative differences apply. However, in 2050 the contribution by contrails is almost twice as large as the contribution from aircraft CO_2 or O_3. Thus, in 2050 for the Fa1 scenario, our best estimate is that aviation RF (without additional cirrus) grows to about +0.19 W m^{-2}, which is 5% of the total anthropogenic radiative forcing anticipated for IS92a of +3.8 W m^{-2} for greenhouse gases plus aerosols (+5.8 W m^{-2} for greenhouse gases alone). This fraction is more than doubled for E-type scenarios (Table 6-1). There is considerable scientific uncertainty in these estimates—a factor of 2 or more at the 67% confidence level—that is separate from the potential error in projecting future scenarios for aviation and IS92a.

Individual RF components in 2050 attributable to the impact of adding a supersonic fleet are shown in Figure 6-15c (see also Table 6-1). The white bars denote the direct RF of HSCTs; the black bars denote the RF from displaced subsonic air traffic. As already discussed, RF from stratospheric H_2O contributes the

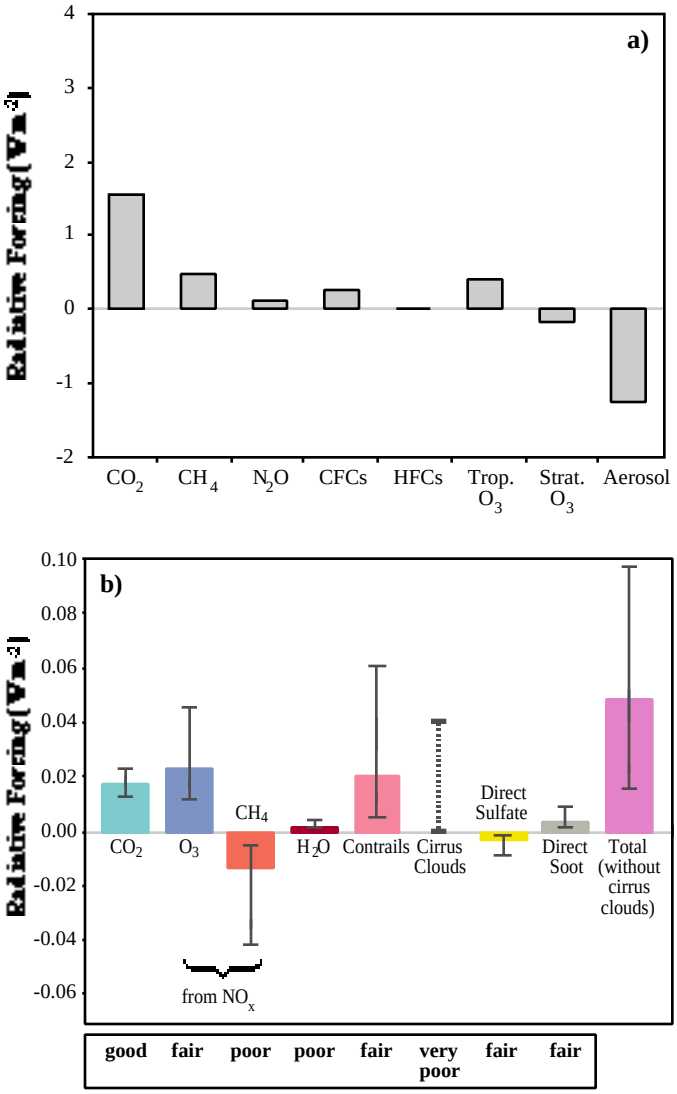

Figure 6-14: Bar charts of radiative forcing from (a) all perturbations in 1990 (from IPCC, 1996) and (b) aviation effects in 1992. Note scale change from (a) to (b). In (b), best estimate (bars) and high-low 67% probability intervals (whiskers) are given. No best estimate is shown for the cirrus clouds; rather, the dashed line indicates a range of possible estimates. The evaluations below the graph are relative appraisals of the level of scientific understanding associated with each component.

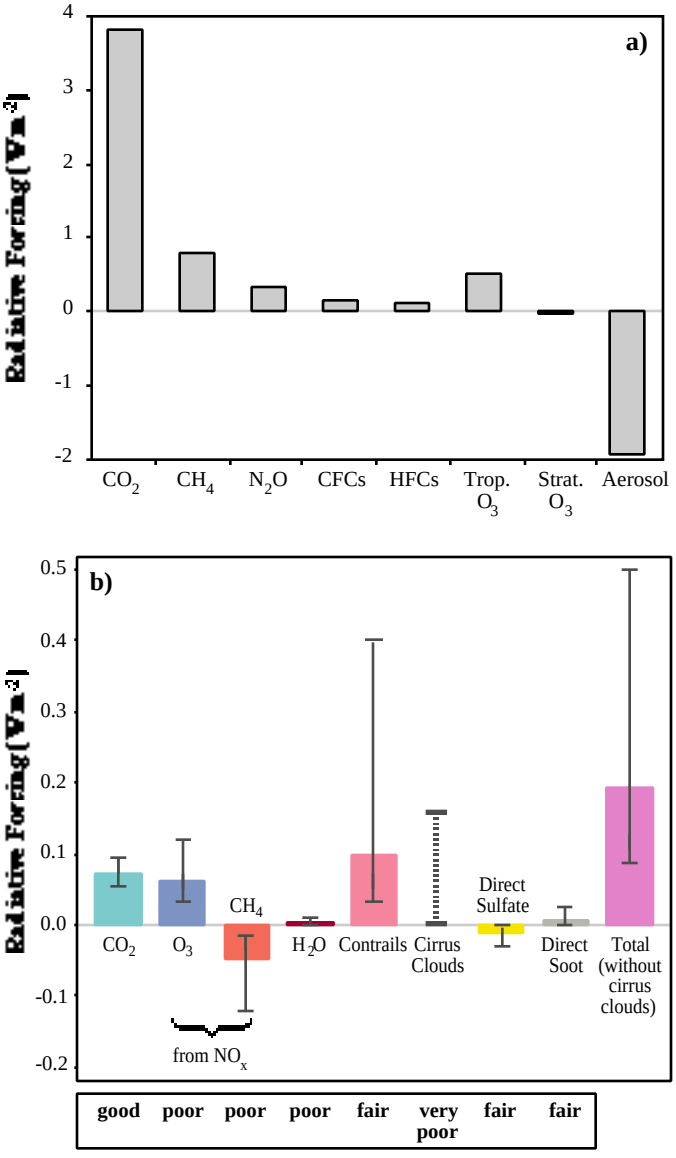

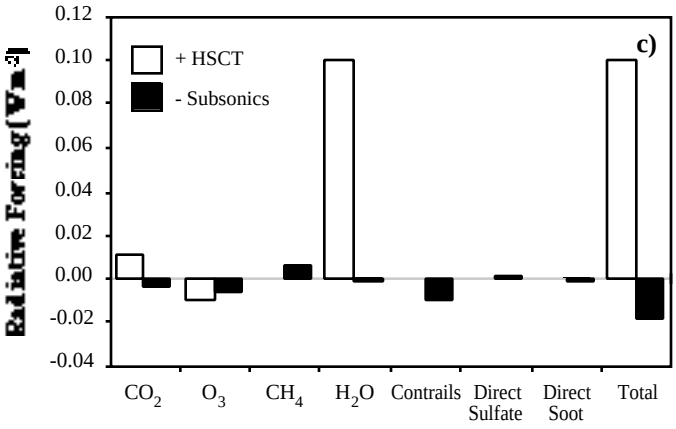

Figure 6-15: Bar charts of radiative forcing in 2050 (a) from all perturbations (from IPCC, 1996), (b) from subsonic aviation (Fa1), and (c) from the additional effect due to supersonic air traffic. Note scale change from (a) to (b) and (c). In (b), best estimate (bars) and high-low 67% probability intervals (whiskers) are given. No best estimate is shown for cirrus clouds; rather, the dashed line indicates a range of possible estimates. The evaluations below the graph are relative appraisals of the level of scientific understanding associated with each component. In (c), white bars denote the direct effect of the supersonic fleet (HSCT1000), whereas the black bars display the change resulting from the displaced subsonic air traffic.

largest component, comparable in magnitude to the big three RFs (CO_2, O_3, contrails) from the subsonic fleet (Figure 6-15b). RFs for the combined fleet (Fa1H) are listed separately in Tables 6-1 and 6-2.

6.6.2. Uncertainties and Confidence Intervals

Throughout this report, we focus on "best estimates" for each component of atmospheric perturbations caused by aircraft and then of subsequent climate forcing or ultraviolet change. We also try to understand the confidence that we have in these estimates using uncertainty ranges deduced in Chapters 2, 3, and 4 and those from the modeling and combining of RF in this chapter.

Uncertainties in estimating aviation's RF values are addressed with a confidence interval (indicated by error bars or whiskers about each best value) and a description ("good," "fair," "poor," "very poor") of the level of scientific understanding of the physical processes, models, and data on which the calculation is based. The confidence intervals shown in Figures 6-14b and 6-15b define a likelihood range such that the probability that the true value falls within the interval is 2/3. The interval and the quality-of-the-science descriptions are, to a large extent, independent measures covering different aspects of uncertainty.

The likelihood range is defined consistently within this report as the 2/3 or 67% probability range. These probability ranges are meant to be symmetric about the best value; hence, the best value is not always the mean of the upper and lower values. In this case, the probability that the value is less than the lower value is 16%, and the probability that it is less than the upper value is 84%. The range between the low and high values is equivalent to the "1-sigma" range of a normal (i.e., Gaussian) probability distribution. Unfortunately, derivation of these confidence intervals lies with the expert judgment of the scientists contributing to each chapter and may include a combination of objective statistical models and subjective expertise. Thus, the 67% confidence intervals do not imply a specific statistical model and, for example, cannot be used to infer the probability of extreme events beyond the stated confidence interval.

The confidence interval in RF stated here combines uncertainty in calculating atmospheric perturbation to greenhouse gases and aerosols with that of calculating radiative forcing. It includes, but is not based solely on, the range of best values from different research groups. For example, the interval for the HSCT(1000) impact on O_3 was derived from high- and low-end calculations using different combinations of atmospheric models and chemical assumptions. The range in RF from these stratospheric O_3 perturbations was expanded further in this chapter to account for the difficulty in calculating RF for stratospheric perturbations. The tropospheric O_3 perturbation from the subsonic fleet (scenario Fa1) was presented with the 67% confidence interval as a factor of 2 higher and lower than the best value. In this case, the RF calculation did not significantly add to the uncertainty because tropospheric perturbations can be more accurately calculated. The confidence interval for aviation-induced CH_4 changes is believed to be about 1.5 times larger (log-scale) than that for tropospheric O_3, but potential errors in both are highly correlated. The confidence interval for contrails is taken directly from Chapter 3; the RF from additional cirrus clouds is highly uncertain and no probability range is given.

The RF uncertainties from different perturbations have been determined by different methods; potential errors in individual components may not be independent of one another, and the error bars may not represent Gaussian statistics. The uncertainty ranges for the totals in Figures 6-14b and 6-15b do represent a 2/3 probability range as for the individual components. The uncertainty estimate for the total radiative forcing (without additional cirrus) is calculated directly from the individual components as the square root of the sums of the squares of the upper and lower ranges. There is a further issue on confidence levels that is not quantified here—namely, the accuracy of representing the climate perturbation by the sum of RF values that are global means.

Overall, addition of the best values for RF provides a single best estimate for the total. The uncertainty ranges for individual impacts can be used to assess whether they are potentially major or trivial components and to make a subjective judgment of confidence in the summed RF.

6.6.3. Aircraft as a Fraction of Total Radiative Forcing

In the aircraft scenarios considered here, the relative amount of aviation fuel burned in 1990 (2.4% of all fossil fuel carbon emissions) would increase by 2050 to about 3% (Fa1) or more than 7% (Eab) depending on projections for air traffic (see Figure 6-16a). For the other scenarios here—with economic assumptions differing from the reference case IS92a, hence a different demand for air transport—these fuel fractions in 2050 may be a factor of 1.5 larger. In comparison, aviation was responsible in 1990 for about 3.5% of total anthropogenic RF. This fraction would grow to about 5% in 2050 for Fa1 and 10% for Eab. Figure 6-16b shows the evolution of aviation RF from 1990 to 2050 for several scenarios as a percentage of total IS92a RF. The climate change forced by aircraft, as measured by the summed RF, is a larger proportion of total RF than indicated by fuel use alone. Thus, aviation is an example of an industry for which the climate impacts of short-lived perturbations such as O_3 and aerosols/clouds must be considered when evaluating the sector as a whole. This effect is also demonstrated by RFI—the ratio of summed RF to CO_2-RF—which is greater than 1 (see Table 6-1).

Each of the demand scenarios has a technology 2 option in which a 25% reduction in EI(NO_x) (corresponding to a 22% reduction in total NO_x emissions) is achieved at an additional fuel cost of about 3.5%. These options are calculated to have very little impact on total RF (Table 6-1) because the reduced O_3-RF is offset by the increased CH_4-RF and the small extra

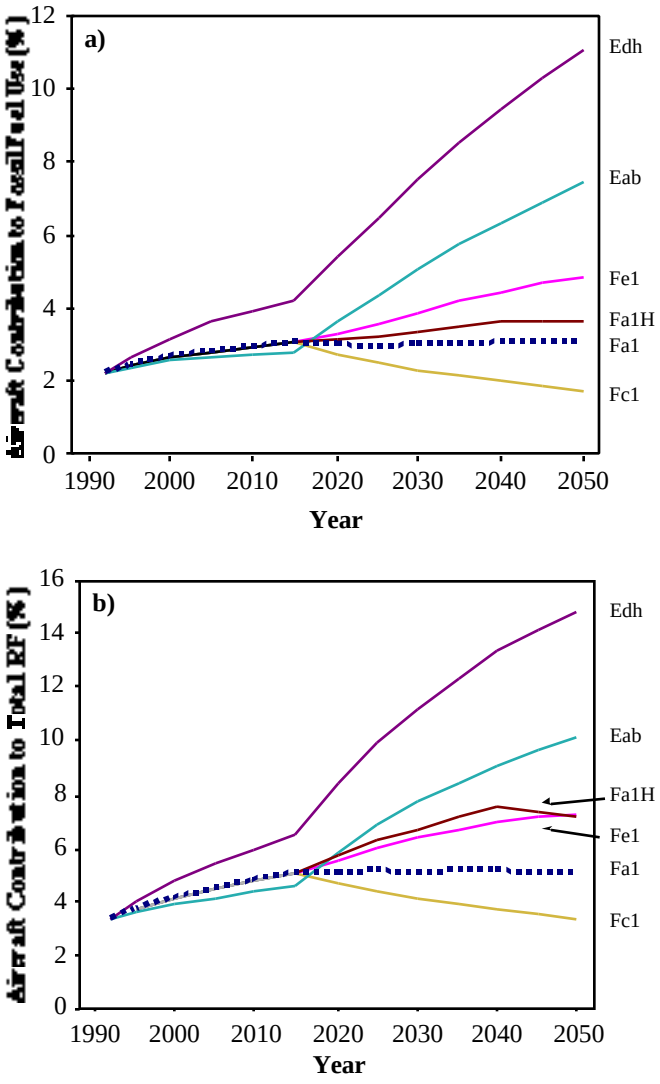

Figure 6-16:(a) Aviation fossil fuel use relative to the IS92a fossil fuel use from 1990 to 2050 for the air traffic scenarios Fc1, Fa1, Fa1H, Fe1, Eab, and Edh; and (b) from aviation as percentage of total radiative forcing (without additional cirrus).

fuel burn (CO_2-RF). If the CH_4 perturbation is tied to the O_3 perturbation as the models now indicate, then the O_3-RF and the CH_4-RF nearly cancel, and efforts at NO_x reduction may not be as effective in reducing RF as previously estimated when only ozone changes were considered. However, these opposing contributions to the radiative imbalance are very non-uniform in geographic extent, and the regional climate response may not simply disappear (see Section 6.5.1). Moreover, the prospect of large and canceling RFs, each with large independent uncertainties, greatly increases the probability of a large residual.

6.6.4. The HSCT Option and Radiative Forcing

The HSCT option of building a fleet beginning in 2015 and capping at 1,000 aircraft in 2040 (scenario Fa1H) has significant impact on total aviation RF, as shown in Figure 6-15c. The addition of HSCT aircraft (+0.08 W m^{-2}) increases RF for scenario Fa1 by a factor of 1.4, becoming comparable to RF for the higher demand scenario Fe1 (see also Figure 6-16b). The HSCT aircraft themselves cause RF of +0.10 W m^{-2}, which is offset only by -0.02 W m^{-2} from displaced subsonic aircraft. This large RF from HSCT aircraft is driven mainly by RF from increased stratospheric H_2O. This single component has a large uncertainty (at least a factor of 3) associated with the calculation of the stratospheric buildup of water and the value of RF. The differential CO_2-RF penalty for HSCT aircraft is only 3% of total aviation RF. In conclusion, the best estimate of RF from HSCTs is about five times as large as RF from the subsonic fleet they replace; however, with the large confidence intervals on O_3 and H_2O, this factor has a very large uncertainty and may range from 0 to 16.

6.6.5. Climate Change

The ranges of aircraft perturbations to climate change examined in this report are, of course, small compared to the overall increase in RF expected throughout the next century. Climate modeling of this transient change over the next 50 years cannot readily evaluate aircraft, or any equally small RF, in terms of specific climate changes because of problems in separating "signal" from "noise." Climate parameters that might be attributed to aircraft, such as the increase in global mean surface air temperature, are calculated here using a simple model consistent with previous IS92a relationships.

The predicted change in global mean surface temperature is shown in Figure 6-17 for total warming in accord with IS92a (solid) and for the case in which all of aviation's contribution to global warming (scenario Fa1) is cut off (dotted line). Of total global warming of 0.9 K anticipated in 2050, about 0.05 K would be attributable to aviation. The Eab case anticipates a larger aviation component (0.09 K). One caveat is that aircraft

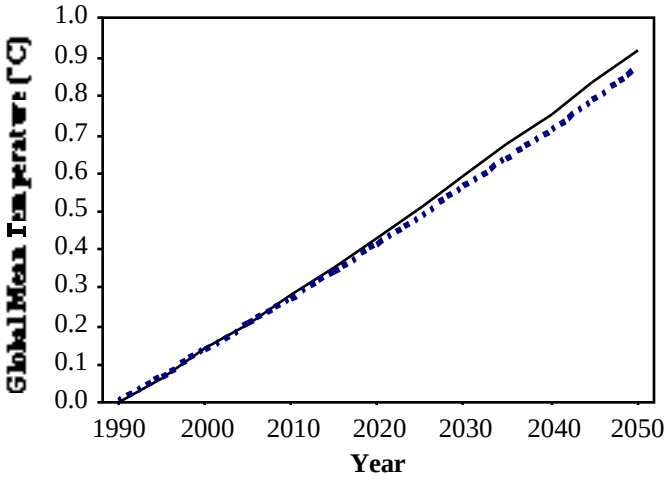

Figure 6-17:Predicted change in global mean surface temperature (K) from 1990 (defined as 0) to 2050 for the IS92a emission scenario (solid line) and for the same scenario without aircraft (Fa1, dotted line).

may produce a different climate signature, one that is not represented by an increase in global mean temperature.

To evaluate individual energy sectors as part of overall climate forcing, it is necessary to compare their summed radiative forcing from all atmospheric perturbations, not just that from their use of fossil-fuel carbon alone. The radiative forcing index—defined here as the ratio of total radiative forcing to that from CO_2 emissions alone—is a measure of the importance of aircraft-induced climate change relative to that from an equivalent sector with the same fossil fuel use but without any effect other than CO_2 (see also Section 6.2.3). In 1992, the RFI for aircraft was about 2.7, with an uncertainty of at least ±1.5. The RFI changes to 3.0 by 2015 then drops to 2.6 for the Fa1 scenario (see Table 6-1). This index ranges from 2.2 to 3.4 in the year 2050 for the various E- and F-type scenarios for subsonic aviation and technical options considered here. The RFI increases from 2.6 to 3.4 with the addition of HSCT aircraft (scenario Fa1H), as a result of the effects of stratospheric water vapor. Thus, aircraft-induced climate change with RFI > 1 points to the need for a complete scientific assessment rather than basing the climate impact on the use of fossil fuel alone. For comparison, in the IS92a scenario, the RFI for all human activities is about 1; for greenhouse gases alone it is about 1.5, and it is much higher for sectors emitting CH_4 and N_2O without significant fossil fuel use.

6.6.6. Aviation and Anthropogenic Change

The overall positive anthropogenic RF today, leading toward global warming, is caused primarily by an increase in anthropogenic emissions of long-lived greenhouse gases, countered in part by short-lived aerosols. Much of this radiative forcing has built up since the industrial revolution. Emissions from aviation are a relatively new contributor to this RF, although they are potentially a growing sector. In evaluating climate change forced by aviation, as well as that by other industrial sectors, the RFI provides a useful indicator. With an RFI of about 3, aviation's role in climate change involves several important climate perturbations beyond that from its release of fossil carbon alone.

This report presents the first thorough IPCC climate assessment of any industrial or agricultural sector. It includes all known climate forcings, many of which are important and not currently represented by indices such as GWP. Comparison of aviation to other industries must await an equally thorough evaluation of the summed effects of human activities by sector that is not available in IPCC (1996) but is anticipated for IPCC's Third Assessment Report in 2001.

The range of technology options that would attempt to reduce the impact of aviation on climate did not significantly change radiative forcing by the year 2050. A lesson taken from the Second Assessment Report (IPCC, 1996, Figure 6a) is that changes in total radiative forcing, even the wide range of emissions for the IS92a-f scenarios, do not appear much before year 2050. Thus, subsequent climate assessments of 21st century options for civil aviation need to carry out projected changes in greenhouse gases and aerosols, and all chemical and climate feedbacks, to the year 2100.

References

Boucher, O. and U. Lohmann, 1995: The sulfate-CCN-cloud albedo effect. A sensitivity study with two general circulation models. *Tellus,* **47B,** 281–300.

Brasseur, G.P., R.A. Cox, D. Hauglustaine, I. Isaksen, J. Lelieveld, D.H. Lister, R. Sausen, U. Schumann, A. Wahner, and P. Wiesen, 1998: European scientific assessment of the atmospheric effects of aircraft emissions. *Atmospheric Environment*, **32,** 2329–2418.

Chou, M.D. and M.J. Suarez, 1994: *An Efficient Thermal Infrared Radiation Parameterization for Use in General Circulation Models.* NASA Technical Memorandum 104606, Technical Report Series on Global Modeling and Data Assimilation, Vol. 3, National Aeronautics and Space Administration, Greenbelt, MD, USA, 85 pp.

Cubasch, U., K. Hasselmann, H. Höck, E. Maier-Reimer, U. Mikolajewicz, B.D. Santer, and R. Sausen, 1992: Time-dependent greenhouse warming computations with a coupled ocean-atmosphere model. *Climate Dynamics*, **8,** 55–69.

Dameris, M., V. Grewe, I. Köhler, R. Sausen, C. Brühl, J.-U. Grooß, and B. Steil, 1998: Impact of aircraft NO_x-emissions on tropospheric and stratospheric ozone. Part II: 3-D model results. *Atmospheric Environment*, **32,** 3185–3200.

Danilin, M.Y., D.W. Fahey, U. Schumann, M.J. Prather, J.E. Penner, M.K.W. Ko, D.K. Weisenstein, C.H. Jackman, G. Pitari, I. Köhler, R. Sausen, C.J. Weaver, A.R. Douglass, P.S. Connell, D.E. Kinnison, F.J. Dentener, E.L. Fleming, T.K. Berntsen, I.S.A. Isaksen, J.M. Haywood, and B. Kärcher, 1998: Aviation fuel tracer simulation: model intercomparison and implications. *Geophysical Research Letters*, **25,** 3947–3950.

Dessler, A.E., E.M. Weinstock, E.J. Hintsa, J.G. Anderson, C.R. Webster, R.D. May, J.W. Elkins, and G.S. Dutton, 1994: An examination of the total hydrogen budget of the lower stratosphere. *Geophysical Research Letters*, **21,** 2563–2566.

Dlugokencky, E.J., K.A. Masarie, P.M. Lang, and P.P. Tans, 1998: Continuing decline in the growth rate of the atmospheric methane burden. *Nature*, **393,** 447–450.

Fleming, E.L., S. Chandra, J.J. Barnett, and M. Corney, 1990: Zonal mean temperature, pressure, zonal wind, and geopotential heights as a function of latitude: COSPAR international reference atmosphere. *Advanced Space Research*, **10**, 1211–1259.

Forster, P.M. and K.P. Shine, 1997: Radiative forcing and temperature trends from stratospheric ozone changes. *Journal of Geophysical Research*, **102,** 841–855.

Fortuin, J.P.F., R. van Dorland, W.M.F. Wauben, and H. Kelder, 1995: Greenhouse effects of aircraft emissions as calculated by a radiative transfer model. *Annales Geophysicae*, **13,** 413–418.

Fuglestvedt, J.S., T.K. Bernsten, I.S.A. Isaksen, H. Mao, X.Z. Liang, and W.C. Wang, 1999: Climatic forcing of nitrogen oxides through changes in tropospheric ozone and methane Global 3D model studies. *Atmospheric Environment*, **33,** 961–977.

Gierens, K., R. Sausen, and U. Schumann, 1999: A diagnostic study of the global distribution by contrails. Part II: Future air traffic scenarios. *Theoretical Applied Climatology,* (in press).

Grant, K.E. and A.S. Grossman, 1998*: Description of a Solar Radiative Transfer Model for Use in LLNL Climate and Atmospheric Chemistry Studies.* UCRL-ID-129949, Lawrence Livermore National Laboratory, Livermore, CA, USA, 17 pp.

Grewe, V., M. Dameris, R. Hein, I. Köhler, and R. Sausen, 1999: Impact of future subsonic aircraft NO_x emissions on the atmospheric composition. *Geophysical Research Letters*, **26,** 47–50.

Grossman, A.S., D.E. Kinnison, J.E. Penner, K.E. Grant, J. Tamaresis, and P.S. Connell, 1997: O_3 and stratospheric H_2O radiative forcing resulting from a supersonic jet transport emission scenario. In: *IRS '96: Current Problems in Atmospheric Radiation* [Stamnes, K. and W.L. Smith (eds.)]. Proceedings of an international radiation symposium, Fairbanks, Alaska, USA, 19–24 August, 1996. A. Deepak, Hampton, VA, USA, pp. 818–821.

Hannegan, B., S. Olsen, M. Prather, X. Zhu, D. Rind, and J. Lerner, 1998: The dry stratosphere: a limit on cometary water influx. *Geophysical Research Letters,* **25,** 1649–1652.

Hansen, J., A. Lacis, D. Rind, G. Russell, P. Stone, I. Fung, R. Reudy, and J. Lerner, 1984a: Climate sensitivity: analysis of feedback mechanisms. In: *Climate Processes and Climate Sensitivity* [Hansen, J. and T. Takahashi (eds.)]. Geophysical Monograph 29, American Geophysical Union, Washington, DC, USA, pp. 130–163.

Hansen, J., A. Lacis, D. Rind, and G. Russell, 1984b: Climate sensitivity to increasing greenhouse gases. In: *Greenhouse Effect and Sea Level Rise* [Barth, M. and J. Titus (eds.)]. Van Nostrand Reinhold Co., New York, NY, USA, pp. 57–78.

Hansen, J., R. Ruedy, M. Sato, and R. Reynolds, 1996: Global surface air temperature in 1995: Return to pre-Pinatubo level. *Geophysical Research Letters,* **23,** 1665–1668.

Hansen, J., R. Ruedy, A. Lacis, G. Russel, M. Sato, J. Lerner, D. Rind, and P. Stone, 1997a: Wonderland climate model. *Journal of Geophysical Research,* **102,** 6823–6830.

Hansen, J., M. Sato, and R. Ruedy, 1997b: Radiative forcing and climate response. *Journal of Geophysical Research,* **102,** 6831–6864.

Harries, J.E., J.M. Russell III, A.F. Tuck, L.L. Gordley, P. Purcell, K. Stone, R.M. Bevilacqua, M. Gunson, G. Nedoluha, and W.A. Traub, 1996: Validation measurements of water vapor from the Halogen Occultation Experiment (HALOE). *Journal of Geophysical Research,* **101,** 10205–10216.

Hasselmann, K., 1993: Optimal fingerprints for the detection of time dependent climate change. *Journal of Climate,* **6,** 1957–1971.

Hauglustaine, D.A. and C. Granier, 1995: Radiative forcing by tropospheric ozone changes due to increased emissions of CH_4, CO, and NO_x. In: *Atmospheric Ozone as a Climate Gas: General Circulation Model Simulations* [Wang, W.-C. and I.S.A. Isaksen (eds.)]. Springer-Verlag, Berlin, Germany, pp. 189–204.

Haywood, J.M. and K.P. Shine, 1997. Multi-spectral calculations of the radiative forcing of tropospheric sulphate and soot aerosols using a column model. *Quarterly Journal of the Royal Meteorological Society,* **123,** 1907–1930.

Haywood, J.M. and V. Ramaswamy, 1998. Investigations into the direct radiative forcing due to anthropogenic sulfate and black carbon aerosol. *Journal of Geophysical Research,* **103,** 6043–6058.

Haywood, J.M., D.L. Roberts, A. Slingo, J.M. Edwards, and K.P. Shine, 1997a: General circulation model calculations of the direct radiative forcing by anthropogenic sulphate and fossil-fuel soot aerosol. *Journal of Climate,* **10,** 1562–1577.

Haywood, J.M., R.J. Stouffer, R.T. Wetherald, S. Manabe, and V. Ramaswamy, 1997b: Transient response of a coupled model to estimated changes in greenhouse gas and sulfate concentrations. *Geophysical Research Letters,* **24,** 1335–1338.

Holton, J.R., P.H. Haynes, M.E. McIntyre, A.R. Douglass, R.B. Rood, and L. Pfister, 1995: Stratosphere-troposphere exchange. *Review of Geophysics,* **33,** 403–439.

IEA, 1991: Table 4: World Demand by Main Product Groups, World Aviation Fuels. In: *Oil and Gas Information: 1988–1990.* International Energy Agency and Organization for Economic Cooperation and Development, Paris, France, 580 pp.

IPCC, 1990: *Climate Change: The IPCC Scientific Assessment* [Houghton, J.T., G.J. Jenkins, and J.J. Ephraums (eds.)]. Cambridge University Press, Cambridge, United Kingdom and New York, NY, USA, 365 pp.

IPCC, 1992: *Climate Change 1992: The Supplementary Report to the IPCC Scientific Assessment.* Prepared by IPCC Working Group I [Houghton, J.T., B.A. Callander, and S.K. Varney (eds.)]. Cambridge University Press, Cambridge, United Kingdom and New York, NY, USA, 200 pp.

IPCC, 1995: *Climate Change 1994: Radiative Forcing of Climate Change and an Evaluation of the IPCC IS92 Emission Scenarios* [Houghton, J.T., L.G. Meira Filho, J. Bruce, H. Lee, B.A. Callander, N. Harris, and K. Maskell (eds.)]. Cambridge University Press, Cambridge, United Kingdom and New York, NY, USA, 339 pp.

IPCC, 1996: *Climate Change 1995: The Science of Climate Change. Contribution of Working Group I to the Second Assessment Report of the Intergovernmental Panel on Climate Change* [Houghton, J.T., L.G. Meira Filho, B.A. Callander, N. Harris, A. Kattenberg, and K. Maskell (eds.)]. Cambridge University Press, Cambridge, United Kingdom and New York, NY, USA, 572 pp.

Isaksen, I.S.A., W.-C. Wang, T. Berntsen, and X.-Z. Liang, 1999: The impact on radiative forcing from aircraft emission (in preparation).

Johnson, C.E. and R.G. Derwent, 1996: Relative radiative forcing consequences of global emissions of hydrocarbons, carbon monoxide and NO_x from human activities estimated with a zonally averaged two-dimensional model. *Climatic Change,* **34,** 439–462.

Jones, P.D., 1994: Recent warming in the global temperature series. *Geophysical Research Letters,* **21,** 1149–1152.

Jones, A., D.L. Roberts, and A. Slingo, 1994. A climate model study of the indirect radiative forcing by anthropogenic sulphate aerosols. *Nature,* **370,** 450–453.

Kattenberg, A., F. Giorgi, H. Grassl, G.A. Meehl, J.F.B. Mitchell, R.J. Stouffer, T. Tokioka, A.J. Weaver, and T.M.L. Wigley, 1996: Climate models—projections of future climate. In: *Climate Change 1995: The Science of Climate Change* [Houghton, J.T., L.G. Meira Filho, B.A. Callander, N. Harris, A. Kattenberg, and K. Maskell (eds.)]. Cambridge University Press, Cambridge, United Kingdom and New York, NY, USA, pp. 285–357.

Lacis, A.A., D.J. Wuebbles, and J.A. Logan, 1990: Radiative forcing of climate by changes in the vertical distribution of ozone. *Journal of Geophysical Research,* **95,** 9971–9981.

Lacis, A. A. and V. Oinas, 1991: A description of the correlated k distribution method for modeling nongray gaseous absorption, thermal emission, and multiple scattering in vertically inhomogeneous atmospheres. *Journal of Geophysical Research*, **96**, 9027–9063.

Li, D. and K.P. Shine, 1995: A4-dimensional ozone climatology for UGAMP models. *UGAMP Internal Report, 35.* Center for Global and Atmospheric Modelling, Department of Meteorology, University of Reading, UK, 35 pp.

Manabe, S. and R.T. Wetherald, 1967: Thermal equilibrium of the atmosphere with a given distribution of relative humidity. *Journal of Atmospheric Science,* **24,** 241–259.

Michaelis, L., 1993: Global warming impacts of transport. *The Science of the Total Environment,* **134,** 117–124.

Mitchell, J.F.B., T.J. Jones, J.M. Gregory, and S.B.F. Tett, 1995: Climate response to increasing levels of greenhouse gases and sulphate aerosols. *Nature,* **376,** 510–504.

Murphy, J.M. and J.F.B. Mitchell, 1995: Transient response of the Hadley Centre Coupled Model to increasing carbon dioxide. Part II: temporal and spatial evolution of patterns. *Journal of Climate,* **8,** 57–80.

Myhre, G., F. Stordal, K. Restad, and I. Isaksen, 1998: Estimation of the direct radiative forcing due to sulfate and soot aerosols. *Tellus,* **50B,** 463–477.

Pollack, J.B., D. Rind, A.A. Lacis, and J.E. Hansen, 1993: GCM Simulations of volcanic aerosol forcing. Part I: Climate changes induced by steady state perturbations. *Journal of Climate,* **6,** 1719–1742.

Ponater, M., S. Brinkop, R. Sausen, and U. Schumann, 1996: Simulating the global atmospheric response to aircraft water vapour emissions and contrails—a first approach using a GCM. *Annales Geophysicae,* **14,** 941–960.

Ponater, M. R. Sausen, B. Feneberg, and E. Roeckner, 1998: *Climate Effect of Ozone Changes Caused by Present and Future Air Traffic.* DLR-Mitteilung 103, Deutsches Zentrum für Luft- und Raumfahrt (German Aerospace Center), Institut für Physik der Atmosphäre, Oberpfaffenhofen and Cologne, Germany, ISSN 0943-4771, 26 pp.

Prather, M.J., 1994: Lifetimes and eigenstates in atmospheric chemistry. *Geophysical Research Letters,* **21,** 801–804.

Ramanathan, V. and R.E. Dickinson, 1979: The role of stratospheric ozone in the zonal and seasonal radiative energy balance of the Earth-troposphere system. *Journal of Atmospheric Science*, **36**, 1084–1104.

Ramaswamy, V. and S.M. Freidenreich, 1997: Anew multi-band solar radiative parameterization. In: *Proceedings of the Ninth Conference on Atmospheric Radiation, February 2–7, 1997, Long Beach, California.* American Meteorological Society, Boston, MA, USA, pp. 129–130.

Rind, D. and P. Lonergan, 1995: Modeled impacts of stratospheric ozone and water vapor perturbations with implications for high–speed civil transport aircraft. *Journal of Geophysical Research,* **100,** 7381–7396.

Rind, D., P. Lonergan, and K. Shah, 1996: Climatic effect of water vapor release in the upper troposphere. *Journal of Geophysical Research,* **101,** 29395–29406.

Rind, D., R. Suozzo, and N.K. Balachandran, 1988: The GISS global climate/middle atmosphere model. Part II: Model variability due to interactions between planetary waves, the mean circulation and gravity wave drag. *Journal of Atmospheric Science*, **45**, 371–386.

Roeckner, E., K. Arpe, L. Bengtsson, M. Christoph, M. Claussen, L. Dümenil, M. Esch, M. Giorgetta, U. Schlese, and U. Schulzweida, 1996: *The Atmospheric General Circulation Model ECHAM-4: Model Description and Simulation of Present-Day Climate.* Report no. 218, Max-Planck-Institut für Meteorologie, Hamburg, Germany, ISSN 0937-1060, 90 pp.

Roeckner, E., J. Feichter, and M. Esch, 1999: Equilibrium climate responses to historical changes in the concentrations of greenhouse gases and aerosols. *Journal of Geophysical Research,* (in press).

Rossow, W.B. and R.A. Schiffer, 1991: ISCCPcloud data products. *Bulletin of the American Meteorological Society*, **72**, 2–20.

Santer, B.D., T.M.L. Wigley, T.B. Barnett, and E. Anyamba, 1996: Detection of climate change and attribution of causes. In: *Climate Change 1995: The Science of Climate Change* [Houghton, J.T., L.G. Meira Filho, B.A. Callander, N. Harris, A. Kattenberg, and K. Maskell (eds.)]. Cambridge University Press, Cambridge, United Kingdom and New York, NY, USA, pp. 407–443.

Sausen, R. and U. Schumann, 1999: *Estimates of the Climate Response to Aircraft Emissions Scenarios.* Report No. 95, Deutsches Zentrum für Luft- und Raumfahrt, Institut für Physik der Atmosphäre, Oberpfaffenhofen, Germany, ISSN 0943-4771, 26 pp.

Sausen, R., B. Feneberg, and M. Ponater, 1997: Climatic impact of aircraft induced ozone changes. *Geophysical Research Letters,* **24,** 1203–1206.

Schumann, U., 1994: On the effect of emissions from aircraft on the state of the atmosphere. *Annales Geophysicae,* **12,** 365–384.

Seinfeld, J.H., 1998: Clouds, contrails and climate. *Nature,* **391,** 837–838.

Shine, K.P., 1991: On the relative strength of gases such as the halocarbons.*Journal of Atmospheric Science*, **48**, 1513–1518.

Shine, K.P., R.G. Derwent, D.J. Wuebbles, and J.-J. Morcrette, 1990: Radiative forcing of climate. In: *Climate Change: The IPCC Scientific Assessment* [Houghton, J.T., G.J. Jenkins, and J.J. Ephraums (eds.)]. Cambridge University Press, Cambridge, United Kingdom and New York, NY, USA, pp. 41–68.

Shine, K.P., Y. Fouquart, V. Ramaswamy, S. Solomon, and J. Srinivasan, 1995: Radiative forcing. In: *Radiative Forcing of Climate Change and an Evaluation of the IPCC IS92 Emission Scenarios* [Houghton, J.T., L.G. Meira Filho, J. Bruce, H. Lee, B.A. Callander, N. Harris, and K. Maskell (eds.)]. Cambridge University Press, Cambridge, United Kingdom and New York, NY, USA, pp. 163–203.

Slingo, A., 1989: AGCM parameterization for the shortwave radiative properties of water clouds. *Journal of Atmospheric Science*, **46**, 1419–1427.

Stamnes, K., W.J. Wiscombe, and K. Jaraweera, 1988: Numerically stable algorithm for Discrete-Ordinate-Method radiative transfer in multiple scattering and emitting layered media. *Applied Optics,* **27**, 2502–2509.

Vedantham, A. and M. Oppenheimer, 1998: Long-term scenarios for aviation: demand and emissions of CO_2 and NO_x. *Energy Policy,* **26,** 625–641.

Wang, W.-C., Y. Zhuang, and R. Bojkov, 1993: Climate implications of observed changes in ozone vertical distributions at middle and high latitudes of the Northern Hemisphere. *Geophysical Research Letters,* **20,** 1567–1570.

Wang, W.-C., X.-Z. Liang, M.P. Dudek, D. Pollard, and S.L. Thompson, 1995: Atmospheric ozone as a climate gas. *Atmospheric Research,* **37,** 247–256.

Washington, W.M. and G.A. Meehl, 1989: Climate sensitivity due to increases CO_2: experiments with a coupled atmosphere and ocean general circulation model. *Climate Dynamics,* **4,** 1–38.

WMO, 1999: *Scientific Assessment of Ozone Depletion: 1998.* Global Ozone Research and Monitoring Project, World Meteorological Organization, (in press).

Wuebbles, D.J., 1996: Three-dimensional chemistry in the greenhouse – an editorial comment. *Climatic Change,* **34,** 397–404.